



# Targeting RNA structures with small molecules

Jessica L. Childs-Disney<sup>1</sup>, Xueyi Yang<sup>1</sup>, Quentin M. R. Gibaut<sup>1</sup>, Yuquan Tong<sup>1</sup>, Robert T. Batey<sup>1,2,3</sup>✉ and Matthew D. Disney<sup>1,3</sup>✉

**Abstract** | RNA adopts 3D structures that confer varied functional roles in human biology and dysfunction in disease. Approaches to therapeutically target RNA structures with small molecules are being actively pursued, aided by key advances in the field including the development of computational tools that predict evolutionarily conserved RNA structures, as well as strategies that expand mode of action and facilitate interactions with cellular machinery. Existing RNA-targeted small molecules use a range of mechanisms including directing splicing — by acting as molecular glues with cellular proteins (such as branaplam and the FDA-approved risdiplam), inhibition of translation of undruggable proteins and deactivation of functional structures in noncoding RNAs. Here, we describe strategies to identify, validate and optimize small molecules that target the functional transcriptome, laying out a roadmap to advance these agents into the next decade.

**Antisense oligonucleotides (ASOs).** Single-stranded DNA or RNA oligonucleotides, including combinations thereof that are chemically modified, that are complementary to the sequence of target RNA and can induce RNase H-mediated degradation or sterically block the ribosome.

**Riboswitch**  
Region of RNA structure located in the 5' leader of bacterial RNAs that undergoes conformational switching upon small-molecule binding to regulate translation.

The first evidence that RNA could be targeted for therapeutic intervention was provided by the discovery of streptomycin in 1944 (REF.<sup>1</sup>) and the subsequent identification of the bacterial ribosome, a macromolecular RNA–protein complex, as the natural product's cellular target<sup>2</sup>. Further insight was provided 20 years later when the first nucleic acid sequence and RNA structure — a tRNA carrying alanine (tRNA<sup>Ala</sup>) — was reported<sup>3</sup>. The key to understanding the role of tRNA in translation was its 3D fold, required for aminoacylation and hence decoding of mRNA sequence into protein. The discovery of catalytic RNAs<sup>4,5</sup> expanded the chemical functions of RNAs far beyond encoding proteins and decoding mRNAs.

The sequence of the human genome further reinforced RNA's contribution to biology, with far fewer canonical open reading frames (ORFs) observed than expected<sup>6</sup>. Indeed, organismal complexity is not correlated with the number of ORFs but instead with the number and diversity of noncoding (nc)RNAs<sup>6</sup> that function in epigenetic regulation<sup>7</sup> and regulate gene expression<sup>8</sup>, particularly during development. Complementarily, genome-wide association studies (GWAS) have defined biological pathways that are dysregulated in disease, elucidating potential therapeutic targets, both RNA and protein. Such data can be leveraged to enable a bench-to-bedside paradigm in which small molecules bind to and deactivate structured RNAs: a patient's genome could be sequenced and compared with GWAS to identify the malfunctioning RNA. The targeted therapy would bind a functional structure within the RNA to short-circuit disease pathways.

Promising therapeutic strategies to target RNA include antisense oligonucleotides (ASOs), CRISPR gene editing and small molecules that recognize RNA structures. ASOs and CRISPR editing have been invaluable to the field of chemical biology. However, translating these technologies to the clinic has been challenging owing to difficulties with delivery and significant adverse reactions<sup>9,10</sup>. Small molecules offer an important alternative with potential for oral bioavailability and blood-brain barrier penetrance, particularly with the wealth of knowledge from medicinal chemistry whereby physicochemical properties can be systematically optimized to improve pharmacokinetics and potency.

Several small molecules that bind RNA structures have been identified that exhibit various modes of action (MOAs), from simple binding to direct cleavage to recruitment of endogenous nucleases (induced proximity). These molecules have been demonstrated to modulate diverse biological processes, such as inhibiting bacterial and viral translation (ribocil and a riboswitch in *Escherichia coli*<sup>11</sup>, 2-aminobenzimidazole derivatives and the hepatitis C internal ribosome entry site (IRES)<sup>12</sup>); inhibiting mRNA translation (synucleozid and α-synuclein<sup>13</sup>); facilitating alternative pre-mRNA splicing (risdiplam<sup>14</sup> and branaplam<sup>15</sup> and survival of motor neuron 2 (SMN2)); and inhibiting microRNA (miRNA) biogenesis (a spermine–amidine conjugate and the miR-372 precursor<sup>16</sup>).

This Review describes foundational methods and strategies to: identify structured, functional RNAs; design and discover lead molecules that bind structured regions; and lead-optimize small molecules, including

<sup>1</sup>Department of Chemistry, Scripps Research, Jupiter, FL, USA.

<sup>2</sup>Department of Biochemistry, University of Colorado, Boulder, CO, USA.

<sup>3</sup>These authors jointly supervised this work:  
Robert T. Batey and  
Matthew D. Disney.

✉e-mail: robert.batey@colorado.edu; mddisney@me.com

<https://doi.org/10.1038/s41573-022-00521-4>

**Internal ribosome entry site (IRES).** RNA structural element typically in the 5' untranslated region that can recruit ribosomes and initiate cap-independent translation.

#### MicroRNA

(miRNA). Short noncoding RNA that has important roles in mediating gene expression by guiding Argonaute proteins to their mRNA target via base pairing to the 3' untranslated region. miRNAs are formed stepwise, first from primary miRNAs to precursor miRNAs by the nuclease Drosha; then from precursor to mature (functional) miRNAs by the nuclease Dicer.

#### Pharmacophore

3D arrangement of a molecule or molecular group that confers bioactivity via interactions with the compound's target.

#### Transcriptome

A landscape of all RNAs transcribed from a genome.

pharmacophore modelling, structure-based design and targeted degradation. Considerations and future directions for the development of small-molecule RNA binders are highlighted.

### Defining RNA structures for small-molecule targeting

#### Determining RNA structure

An accurate model of RNA structure is key to the design or discovery of small molecules that modulate its function. Computational methods can model RNA structure from sequence, including free energy minimization and phylogenetic comparison. Free energy minimization uses experimentally derived thermodynamic parameters to predict RNA structures<sup>17</sup>, outputting the minimum free energy structure, assumed to be the functional structure, as well as suboptimal structures. The total free energy of an RNA structure is calculated by summing the free energy of each substructure in the system, such as base pairs, bulges and loops. Dynamic programming algorithms<sup>18,19</sup>, the basis of programs such as mFold<sup>20</sup>, RNAfold<sup>21</sup> and RNAStructure<sup>22</sup>, incorporate these experimentally determined thermodynamic parameters, predicting accurately ~70% of the base pairs for RNAs <700 nucleotides long.

Experimental constraints can be integrated into the algorithms to improve the reliability of the prediction<sup>23</sup>. Unpaired nucleotides can be identified both *in vitro* and *in vivo* using chemical modification by dimethyl sulfate (DMS<sup>23</sup>) or by selective 2'-hydroxyl acylation analysed by primer extension (SHAPE)<sup>24–29</sup>. Chemical modification either pauses reverse transcriptase (RT), causing truncation of the cDNA (an 'RT stop'), or induces a mutation, both of which can be read out by high-throughput sequencing. These sites of modification restrain secondary structure predictions in which the extent of modification is correlated with an energetic penalty for a nucleotide to be paired. Transcriptome-wide DMS and SHAPE probing techniques greatly expanded knowledge of the overall RNA structural profiles in cells and enabled investigation of RNA conformational changes under various biological conditions<sup>24–26</sup>. Although these experimental constraints refine the predicted models, they do not provide information about the 3D fold of the RNA, as provided by X-ray crystallography, NMR spectrometry and cryo-electron microscopy (cryo-EM).

Phylogenetic comparison also provides insight into RNA structure, where genetic differences that preserve secondary structure (covariations: for example, an AU base pair is replaced with GU or GC) can elucidate structure, and conservation suggests selective pressure to retain a functional structure<sup>30,31</sup>. Covariation-based structural prediction of many RNA structures is highly accurate, as determined by comparison with crystal structures<sup>32,33</sup>. However, owing to the large dataset required and the complexity of the analysis, automated covariation-based prediction methods remain challenging. Phylogenetic comparison has been coupled with other prediction methods, either in sequence or co-processed, including homology modelling, free energy minimization and chemical modification to improve accuracy<sup>34–36</sup>, which relies on the quality of alignment and sequence availability.

The folding of RNA is hierarchical, and RNAs can form tertiary structures. Information about RNA 3D structure is especially valuable in uncovering the functional mechanism of RNAs and identifying druggable targets. Although 3D prediction methods are still in their infancy compared with those for proteins, currently available programs, including FARFAR2 (REF.<sup>37</sup>) (RNA analogue of ROSETTA for protein prediction), MC-Fold/MC-Sym<sup>38</sup> and iFoldRNA<sup>39</sup>, have shown promising results for predicting 3D structures from sequence. Scoring functions that estimate the accuracy of prediction results in which the native structure is unknown have also been developed, such as Rosetta<sup>37</sup>, RASP<sup>40</sup> and ARES<sup>41</sup>. With the implementation of machine learning techniques, ARES outperforms the other two approaches. Root-mean-square deviation (r.m.s.d.) analysis of predicted structures to known crystal structures demonstrated the power of this approach<sup>41</sup>.

Biophysical methods such as NMR spectroscopy, X-ray crystallography and cryo-EM have also been extensively used to determine RNA structure<sup>42–44</sup>. NMR spectroscopy studies also provide information about structural dynamics. Although cryo-EM is typically used to study the structure of molecules of large molecular weight, considerable effort is being exerted to develop approaches that can access smaller RNA structures, for example, as recently reported for a small riboswitch (<40 kDa)<sup>45</sup>. Computationally assisted cryo-EM has also been introduced to determine the global conformation of RNA molecules, although it does not provide atomic-level resolution<sup>46</sup>.

#### Assessing the quality of RNA structural predictions

Many algorithms have been developed that predict RNA structure. However, without a known structure, it is hard to assess the reliability and accuracy of the prediction, which has been addressed by development of various statistical methods.

Partition function calculations have been incorporated into various structure prediction programs, including RNAfold<sup>21</sup>, Sfold<sup>47</sup> and CONTRAfold<sup>48</sup>. A partition function contains all of the thermodynamic information for a system and quantifies the probability of the predicted structure or substructure therein. Statistics have also been applied to phylogenetic comparisons such as R-scape, which measures the statistical significance of evolutionary covariation, indicative of functionality<sup>49</sup>. Although R-scape improved the annotation of the consensus structure in 5S rRNA from the Rfam<sup>50</sup> database, it did not find significant covariation in the long noncoding (lnc)RNAs HOX antisense intergenic RNA (HOTAIR), steroid receptor RNA activator (SRA) or X-inactive specific transcript (Xist)<sup>49</sup>, although plausible structures have been predicted by other computational methods<sup>51–53</sup>. The lack of functional structures in these lncRNAs did not stem from the lack of variance in the phylogenetic tree<sup>54</sup>, nor does it imply that these lncRNAs do not fold. Instead, they likely form dynamic structures stabilized in the context of other interacting partners, pointing to the importance of knowing the limitations of predictive methods and of experimental validation.

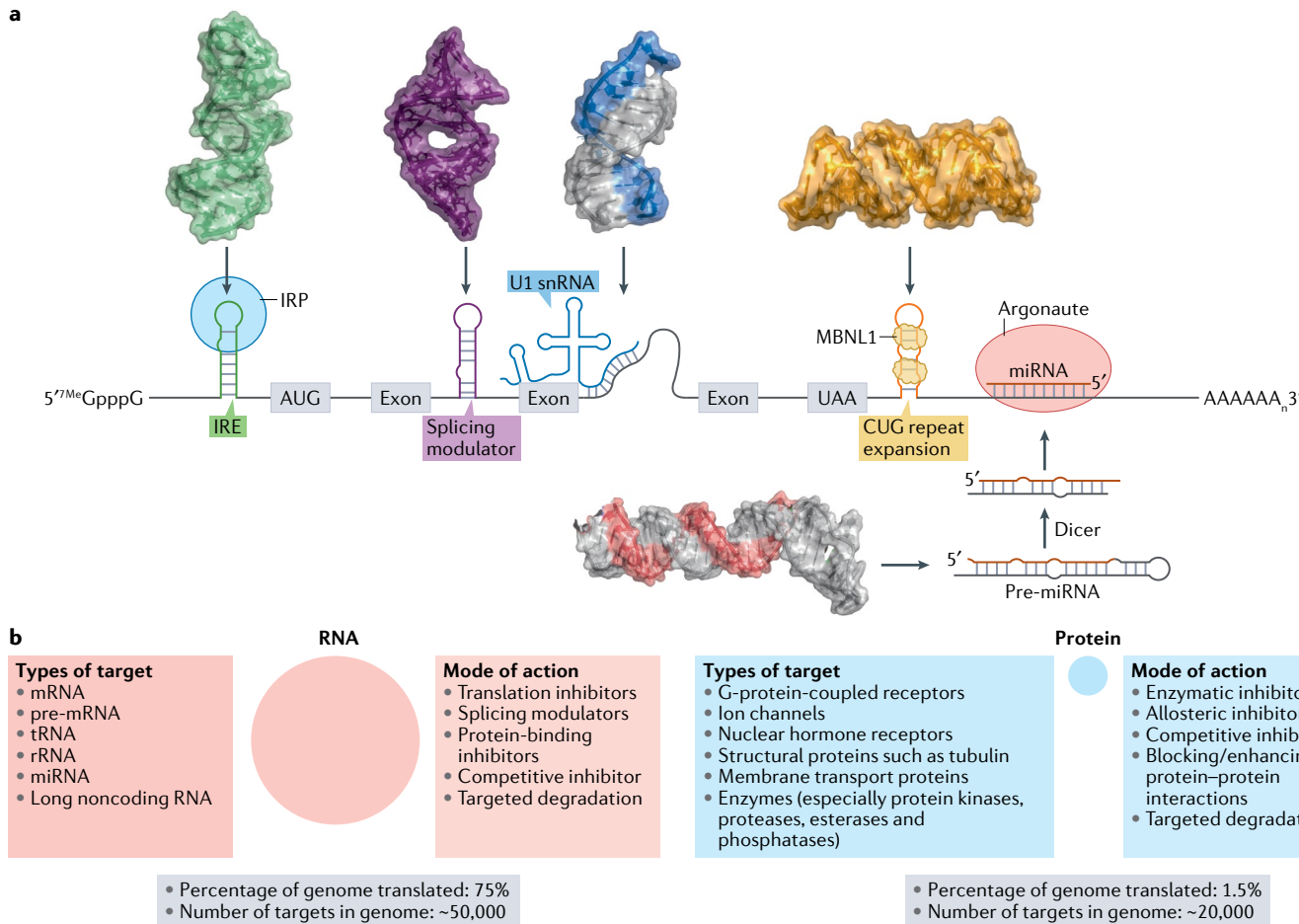


**Fig. 1 | Human RNAs regulate key biological processes, and their functions are driven by their structures. a |** Examples of structured regions of RNA with important biological functions include IRE (iron-responsive element; translational regulation), splicing modulators (alternative pre-mRNA splicing including those that interact with U1 small nuclear RNA (snRNA)), RNA repeat expansions (aberrant gain-of-function; microsatellite disorders) and Drosha and Dicer processing sites in microRNA (miRNA) precursors. PDB codes: IRE (PDB: 1NBR), intron splicing junctions (PDB: 6VA1, 6HMO), RNA repeat (PDB: 1ZEV). The model of the miRNA structure can be found in REF.<sup>108</sup>. **b |** Comparison of RNA and protein as therapeutic targets. Approximately 75% of the human genome is transcribed into RNA, while 1.5% is translated into protein. Common types of drug target and their modes of action are also listed.

Collectively, these methods demonstrate that predicted structures must be viewed through the lens of statistical power and/or rigour and tempered with in-depth dissection of their biological function. That is, these predictions are hypotheses until further validated.

#### Defining functional RNA structures in the transcriptome

Functional RNA structures can be found throughout a transcript from the 5' end to the 3' end, from untranslated regions to ORFs (FIG. 1). Although data suggest that ORFs are less structured than other regions<sup>55–57</sup>, highly structured coding sequences have been discovered<sup>58,59</sup>. Functional structures can be identified computationally (below) or experimentally by using ASOs that sterically block a functional structure<sup>60</sup> or by mutational analysis<sup>61</sup>.

Although many RNA structural prediction methods can provide accurate models of RNA secondary structure, they do not predict functionality. Functionality can be predicted by identifying regions of structure that are unusually thermodynamically stable compared with random

sequences. The hypothesis is that these stable structures are evolutionarily retained because of selective pressure. ScanFold, a scanning window approach, uses these principles to identify potentially functional structures<sup>62</sup>, accurately predicting known functional viral structures as well as predicting potential new functional structures in viral and human transcriptomes<sup>63,64</sup>.

Structural conservation and genetics can also indicate function. For the former, structural motifs that are evolutionarily conserved across species likely have a biological function<sup>30,31</sup>; for the latter, genetic mutations can cause gain or loss of function. Perhaps the best example of evolutionary conservation of structure and function is rRNA. Indeed, highly conserved structures can be found in bacteria (riboswitches), viruses (IRESs) and humans (IRESs, splicing regulatory elements).

The hunt for targetable, functional RNA structures, particularly in the human transcriptome, has only just begun. Thus far, RNA structures that have been effectively targeted with small molecules (binding produces a downstream biological response), participate

**Splicing modulators**  
Small molecules or proteins that are capable of directing RNA splicing by inducing inclusion or exclusion of exons.

### Box 1 | Commonalities amongst small molecules that bind RNA

Ideally, small molecules that bind RNA targets would be drug-like and orally bioavailable, as defined by their physicochemical properties. Indeed, analysis of the physicochemical properties of drugs that target proteins have provided guidelines for drug development, such as the Lipinski 'rule of five'<sup>275</sup>. RNA, however, is very different from proteins in terms of its chemical composition, its highly electronegative surface potential and its limited buried surface area. It is therefore reasonable to infer that RNA-binding small molecules will have unique properties that do not necessarily fall into traditional rule of five guidelines. Notably, new modalities such as chimeric compounds that target proteins for degradation have many drug discovery efforts lying 'outside of the rule of five'. Various studies have identified privileged scaffolds and chemotypes that confer affinity for RNA, for example, indole, 2-phenylindole, 2-phenyl benzimidazole, 2-phenylimidazole, methylpyrimidine-2,4-diamine and others<sup>67,78,281,282</sup>. Further, comparison of the physicochemical properties of RNA-binding molecules with those of FDA-approved drugs available in DrugBank revealed distinct differences<sup>109,283,284</sup>. In particular, RNA-binding compounds on average have lower octanol–water partition coefficients (LogPs) than protein-binding compounds (ranges from two separate analyses:  $0.16 \pm 5$  versus  $2.0 \pm 3.5$  (REF.<sup>109</sup>) and  $1.02$  versus  $1.78$  (REF.<sup>283</sup>), respectively), greater topological polar surface areas ( $156 \pm 118$  versus  $92 \pm 144 \text{ \AA}^2$ <sup>109</sup>), more hydrogen bond donors ( $5.2 \pm 5$  versus  $2.0 \pm 4$ ) and acceptors ( $8.6 \pm 6$  versus  $5.0 \pm 6$ <sup>109</sup>), and more heteroatom-containing aromatic rings ( $2.16$  versus  $1.25$ )<sup>283</sup>. An analysis by the Hargrove laboratory suggested that the shape of RNA binders is generally rod-like<sup>283</sup>. Given the infancy of RNA targeting, these comparisons will likely change as new molecular interactions and activities are catalogued.

A previous analysis investigated the interplay between small-molecule affinity, target complexity and quantitative estimate of drug-likeness (QED)<sup>186</sup>. QED, a metric of compound quality, evaluates how closely each physicochemical property of a small molecule, measured on different scales, reflects the ideal value and combines them into a single score<sup>285</sup>. The analysis suggested that the complexity of the RNA target scaled with the affinity for the targets and that drug-like chemical matter emerged when the target RNA structure became more complex<sup>186</sup>. As there is still much to be understood about the interactions at play that confer high-affinity binding, selectivity and bioactivity, the field will need to continue to revise its view on the properties, including drug-likeness, of RNA-targeted small molecules that are important and further determine whether these properties are target- or target class-dependent. However, a few guideposts have been established. For example, traditional drug-like chemical matter is likely useful for RNAs that adopt complicated binding pockets, that is, those that appear riboswitch-like or protein-like. Notably, complexity should not be confused with uniqueness. Kinase inhibitors bind to an ATP-binding pocket formed by a complicated molecular interaction network. However, they are not unique folds, making the development of selective kinase inhibitors challenging<sup>286</sup>. Thus, although an RNA may form a complex structure, it does not necessarily indicate a priori that a selective small molecule can be designed or discovered. In other cases, where the RNA is locally structured (a common occurrence for mRNAs, for example), the lack of buried surface area (in comparison with a complex structure) to drive selective interactions could be overcome by binding to multiple structures within an RNA target simultaneously with a single molecule. Although such compounds may be outside of the rule of five, they can be optimized into orally bioavailable medicines.

in biomolecular interactions with proteins including the ribosome, other RNAs and DNA. Identifying a functional RNA structure only addresses half of the RNA-targeting problem. The other half is discovering or designing chemical matter that selectively binds to the functional structure.

#### Factors that affect the selectivity of small molecules targeting RNA

Ideally, a small molecule would be completely selective for its RNA target, but in practicality that is likely not required or even achievable. Historically, selective recognition of RNA by small molecules was thought intractable, owing to its perceived lack of structural diversity with only four building blocks, its anionic backbone and the lack of success in high-throughput screening campaigns. Selective recognition is possible as our

fundamental understanding of the RNA structures that are targetable and the chemotypes that bind RNA has evolved, alongside advances in RNA structure modelling that provide insight into the functionality of structures.

Binding selectivity and functional selectivity are distinct. Several factors have been identified that drive the cellular (functional) selectivity of ligands that target RNA, including the uniqueness of the structure in the transcriptome, expression of the target compared with off-targets, the relative affinity of the small molecule for on- and off-targets, accessibility of the target site and the functionality of the binding site, where binding to non-functional sites is biologically silent. Regarding target expression, if two or more RNAs have the same binding site, the more highly expressed target will be more occupied by the compound. In the same vein, if two or more RNAs have different structures ligandable by the same compound, the most occupied target will be a composite of relative affinity and expression level. In cases where selectivity is not sufficient, compounds can be designed that target multiple sites within an RNA target simultaneously, thus overcoming the limitations of structural degeneracy (a structure is not unique in the transcriptome).

A few studies have completed transcriptome- and proteome-wide studies that provide insight into the selectivity of RNA-targeting small molecules. These studies have shown that small molecules can exert selective effects across the transcriptome and proteome. Notably, the observed changes and selectivities are similar to those observed for oligonucleotides<sup>65</sup>. An analogue of the FDA-approved drug risdiplam, which binds to an RNA–protein manifold not solely an RNA, is selective, altering the levels of 12 of 11,174 transcripts and altering the alternative splicing of a subset of mRNAs, including the desired target<sup>66</sup>. As observed for small molecules that target proteins, the off-targets for RNA-targeting small molecules could be other RNAs, DNA or proteins. Thus far, it appears that the scaffolds that bind to RNA are different from those that bind to proteins (BOX 1), as also indicated by the lack of success in identifying selective RNA binders from small-molecule libraries designed for proteins.

#### Strategies to identify small-molecule RNA binders

##### Target-centric approaches

Various approaches can be used to find small molecules that bind RNA structures in vitro, including fluorescence-based assays, fluorescence resonance energy transfer (FRET)-based approaches<sup>67–70</sup> and dynamic combinatorial screening<sup>71</sup>. The methods described below are target centric, that is, the small molecule's only choice for binding is a single or a few targets. As with any primary screening assay, secondary analyses are required to identify selective binders. For all fluorescence-based assays described below, care must be taken, as many compounds can interact with the dyes themselves or have emission properties that overlap with the fluorophores.

**Affinity mass spectrometry.** Affinity selection mass spectrometry (AS-MS) is a label-free method that allows the direct identification of target–ligand complexes by mass spectrometry after separation from unbound ligands

##### Functional selectivity

A metric that compares the effect of a compound on the biological activity of the desired target versus its effect on other targets.

##### On- and off-targets

An on-target is the biomolecule that a compound is designed to modulate the function of; an off-target is unintendedly modulated by the small molecule.

by size-exclusion chromatography<sup>72,73</sup>. Used widely for proteins<sup>74</sup>, it has only been recently adopted for RNA targets<sup>75,76</sup>. A variant of AS-MS, named automated ligand identification system (ALIS), uses indirect detection of a target–ligand interaction by dissociating the formed complex before liquid chromatography–mass spectrometry (LC-MS) analysis to identify the bound ligand<sup>74–76</sup> (FIG. 2a). In one example of the use of ALIS, synthetic ligands that bind the flavin mononucleotide (FMN) riboswitch were identified<sup>75</sup>. One challenge associated with AS-MS is the requirement of long small-molecule residence times, such that the complex is still intact after size-exclusion chromatography.

**Fluorescence-based assays.** Another high-throughput assay relies on displacement of a fluorescent dye or compound by a small molecule of interest. Although originally developed to study the binding of DNA structures<sup>77</sup>, it has also been applied to RNA targets by displacement of the fluorescent dye TO-PRO-1 (REFS. <sup>78,79</sup>) (FIG. 2b), as well as others<sup>79–82</sup>. An extension of this dye displacement method is an assay with turn-on fluorescence that uses a known fluorescent or fluorescently labelled binding small molecule and an RNA of interest that is labelled on the 5' or 3' end with a quencher<sup>70</sup>.

Another way to assess small-molecule binding can be carried out by replacing an adenine residue with the fluorescent mimic 2-aminopurine (2-AP)<sup>83</sup>. The fluorescence of 2-AP depends on its microenvironment, which changes upon small-molecule binding (FIG. 2b). This 2-AP assay was originally developed to study the binding of aminoglycosides to bacterial rRNA and the effect of binding on A-site dynamics<sup>84</sup>, but has been extended to other targets<sup>70,85,86</sup>. Notably, the position of the 2-AP substitution within the RNA should be carefully chosen to ensure a strong signal. For small RNAs, this can be accomplished by simply substituting each adenine residue. For longer RNAs, such as riboswitches, SHAPE can be used to elucidate where large conformational changes occur upon ligand binding, and hence the optimal position (or positions) for 2-AP substitution<sup>85,86</sup>.

Many bioactive small molecules have been identified that bind RNAs participating in bimolecular interactions with proteins. To measure inhibition of formation of an RNA–protein interaction or disruption of a pre-formed complex by a small molecule, fluorescence and FRET assays have been developed, particularly for HIV-1 Tat-transactivation response (TAR)<sup>87–89</sup> and for RNA repeat expansions–RNA-binding proteins<sup>69,90</sup>. Labels on the RNA and protein are FRET pairs, and disruption or inhibition of the complex reduces the observed FRET signal (FIG. 2b). Small molecules that bind either the protein or the RNA can reduce FRET, and thus additional investigation is required to confirm that the small molecule binds the RNA as intended.

**Microarray-based screening.** Small-molecule microarrays (SMMs), created by delivery of minute amounts of compounds to glass slides in a spatial array, were initially used to interrogate protein binding<sup>91–94</sup> and later extended to study the binding of aminoglycosides to the rRNA A-site<sup>95</sup> and how binding is affected by aminoglycoside

modification by resistance enzymes<sup>96</sup>. SMMs have now been used to screen a wide variety of compounds and RNA targets<sup>97–103</sup> (FIG. 2c). One advantage of SMMs is that only a small amount of the small molecule is needed to complete a screen and many thousands of interactions can be profiled at once. Compounds are typically covalently attached to the array. Notably, binding to a surface can be quite different from binding in solution. Small molecules can also be non-covalently attached to agarose-coated microarray surfaces by adsorption<sup>104</sup>. Although this method can be broadly applied to many compounds<sup>104</sup>, not all compounds adhere to surfaces.

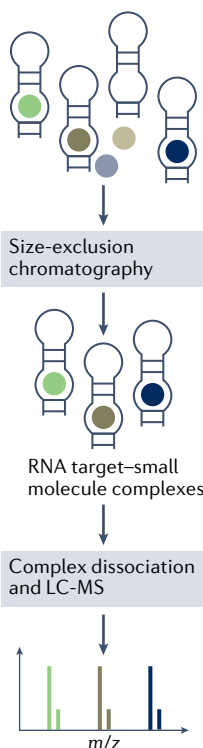
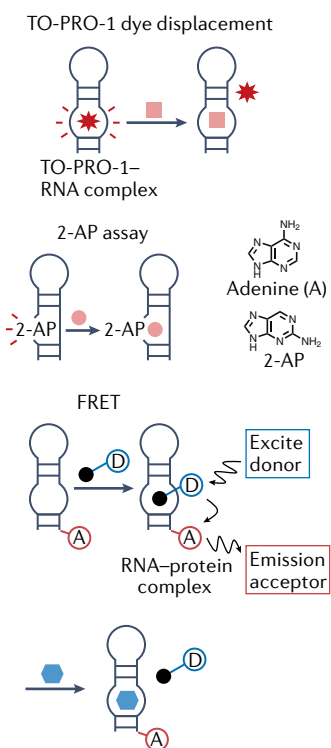
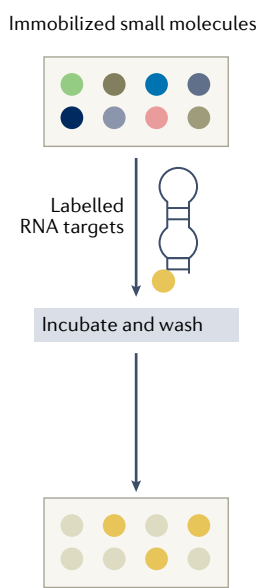
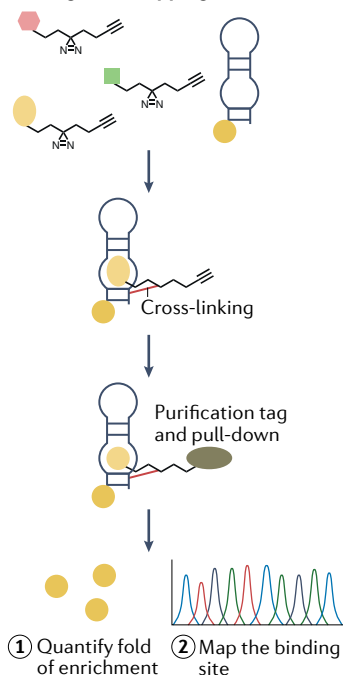
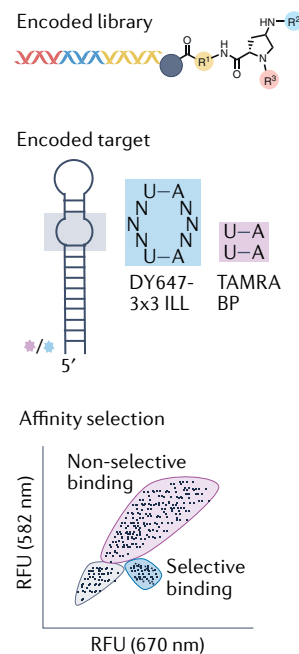
**Fragments.** Fragment-based ligand discovery uses libraries of low-molecular-weight compounds to efficiently explore chemical space that might bind the target of interest (FIG. 2d). Although fragments can be screened for binding, such as by NMR spectroscopy (as demonstrated to identify a fragment that binds severe acute respiratory syndrome coronavirus 2 (SARS-CoV-2)<sup>105</sup>), these interactions are often difficult to detect as they are low affinity and have short residence times. To overcome these limitations, small-molecule fragments have been functionalized with photoaffinity groups (fully functionalized fragments; FFFs) that enable capture and identification of bound targets, first applied to proteins<sup>106,107</sup> and later to RNA<sup>105,108</sup>. Low-molecular-weight fragments are ideal for a modular assembly approach in which two fragments are tethered together to bind two structural elements in an RNA target simultaneously, as favourable physicochemical properties can be maintained (discussed below).

**DNA-encoded compound libraries.** DNA-encoded compound library (DEL) technology is a powerful method to explore chemical space that binds a target biomolecule either in solution or on the solid phase. A DEL is synthesized on beads by split and pool in an iterative process in which one of many building blocks is conjugated and its identity is encoded in a short DNA tag that is ligated to the bead. Compound-functionalized beads are screened for binding typically to a fluorescently labelled target, often in the presence of an off-target that is differentially labelled (FIG. 2e). For RNA targets, a counter-screen can be completed by using an RNA in which the desired binding site has been mutated, akin to mutations for binding analyses (FIG. 2e). For example, a bulged nucleotide could be converted into a base pair or a different bulge, the closing base pairs could be altered and so on. Beads that bind the desired target but not the off-target decoy can be analysed and sorted by flow cytometry. Deep sequencing of the beads identifies the binding compound. Because of the potential of nonspecific binding of the encoding DNA tag, nucleic acids and their binding proteins have been avoided. Thus far, the DEL technology has been applied only twice to nucleic acid targets: RNA<sup>109</sup> and highly structured DNA G-quartets<sup>110</sup>.

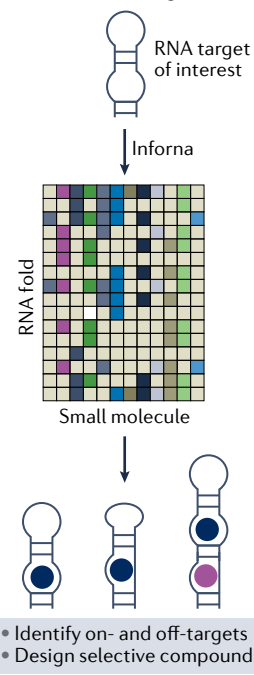
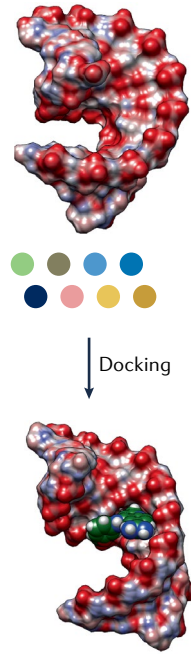
#### Designing small-molecule RNA binders

Rather than screening for chemical matter, RNA binders have been designed using selection-based methods that define the preferred targets of RNA-binding small molecules and structure-based design.

## Methods to identify chemical matter that binds RNA

**a ALIS****b Fluorescence-based assay****c Microarray-based screening****d Fragment mapping****e DNA-encoded chemical library**

## Methods to design chemical matter that binds RNA

**f Inforna mining****g Structure-based design**

**Defining binding landscapes.** A selection-based platform, 2D combinatorial screening (2DCS), defines the binding landscape of an RNA-binding small molecule. Small molecules displayed on a microarray select their preferred RNA partners from an RNA library displaying

a randomized region in a discrete secondary structure pattern<sup>111</sup>. The selection experiment is completed under stringent conditions in the presence of a large excess of competitor oligonucleotides that mimic regions common to all members of the library, restricting binding

**Fig. 2 | Methods to identify or design small-molecule RNA binders.** **a–c** | Methods to identify small molecules that bind RNA. **a** | Automated ligand identification system (ALIS) is a liquid chromatography–mass spectrometry (LC–MS) method. An RNA target is incubated with a library of small molecules. Unbound ligands are removed by size-exclusion chromatography and then bound ligands are identified by LC–MS. **b** | Fluorescence-based assays rely on a change in fluorescence upon small-molecule binding to the RNA target. This could be achieved by: displacing a non-selective RNA-binding dye (top); changing the microenvironment of a fluorescent nucleotide analogue (middle); or disrupting donor–acceptor pairs in a fluorescence resonance energy transfer (FRET)-based assay (bottom). **c** | Microarray-based screening in which a panel of small molecules is pinned to an array surface and incubated with labelled RNA targets, followed by washing and imaging to identify target-binding compounds. **d** | Compounds functionalized with a cross-linking module (such as diazirine or chlorambucil) and a pull-down tag (such as alkyne or biotin) can be screened against labelled RNA targets by using Chem-CLIP (chemical cross-linking and isolation by pull-down) to identify RNA binders and to map the binding sites. **e** | Identification of RNA-binding small molecules from a DNA-encoded library (DEL). The library is synthesized on beads, and each building block added during the synthesis is encoded with a DNA tag. The DEL is screened simultaneously for binding to the target of interest and a related RNA to which binding is undesired. The two RNAs are labelled with different fluorophores, and selective binders from the DEL can be identified and isolated by flow cytometry. **f,g** | Methods to design small molecules that bind RNA. **f** | Infora is a lead identification strategy in which the structures present in a cellular RNA are compared with a database of experimentally determined RNA–small molecule interactions. Overlap affords lead targets and lead small molecules. **g** | Structure-based design of small molecules relies on a model of the structure of the RNA or of the RNA–ligand complex. Both can be used in docking studies while the latter can be used to guide modifications that improve interactions between the RNA and the small molecule. 2-AP, 2-aminopurine; RFU, relative fluorescence units.

interactions to the randomized region. Fully paired DNA and RNA oligonucleotide competitors or tRNAs are also often used to increase the stringency of the selection. Selected RNAs are analysed by RNA sequencing (RNA-seq)<sup>112,113</sup>, followed by rigorous statistical analysis of the enrichment of an RNA by the small molecule<sup>114</sup>. Statistical significance scales with affinity such that the more significant the enrichment of the RNA, the more tightly it binds to the small molecule. This analysis affords a binding landscape, or molecular fingerprint, for each small molecule, where a selective small molecule has few RNAs with statistically significant enrichment and a promiscuous one has many. These binding landscapes inform the ideal target for a small molecule and potential off-targets. Cellular RNA targets can be computationally compared with these molecular fingerprints to inform small-molecule design, as in the lead identification strategy Infora<sup>65</sup> (FIG. 2f). Infora outputs the targetable sites present in a cellular RNA and the rank order of potential small-molecule binders. This approach has been implemented in both a target-centric and a target-agnostic fashion<sup>65</sup>.

**Structure-based design and docking.** First employed for protein targets, structure-based design and docking have enabled the discovery and the optimization of lead compounds for RNA targets<sup>115–121</sup> (FIG. 2g). Using well-defined RNA structures, typically elucidated by NMR spectroscopy, small molecules can be designed to fit within binding pockets. Further, NMR studies also enable the prediction of dynamic ensembles of RNA conformations computationally, including short-lived, non-functional species<sup>120–125</sup>. Small-molecule libraries can then be docked into these ensembles to screen small molecules for selective RNA binding *in silico*<sup>121,126</sup>. The significant limitations of these approaches are the quality

of the RNA structure, as highly accurate structures are difficult to generate by NMR spectroscopy, as well as the docking programs themselves. Interestingly, an NMR method was recently developed to study conformational biases in HIV-1 TAR and Rev responsive element (RRE) RNAs<sup>120</sup>. A series of mutations were made to each RNA, and the effect on conformational equilibria was measured by NMR spectroscopy. These spectral studies can estimate the percentage of the RNA folded into a non-functional fold, confirmed by studying the cellular activity of the RNA mutants<sup>120</sup>.

**Phenotypic screening.** Phenotypic screening is a strategy to identify compounds that affect pathways associated with a specific phenotype and therefore require no knowledge of the MOA or target. These assays design a screen around a biological process, for example, alternative pre-mRNA splicing, inhibition of translation, derepression of protein targets and bacterial growth. Assays completed in mammalian cells typically use generation of either luciferase or a fluorescent protein as a readout. Two small molecules that modulate splicing were discovered from phenotypic screens, the FDA-approved risdiplam<sup>66</sup> and branaplam<sup>15</sup> (currently in phase II clinical trials) for the treatment of spinal muscular atrophy (SMA)<sup>15</sup>.

Although phenotypic screens have been executed successfully, challenges remain, largely because the approach is target agnostic. Despite the fact that target validation and mechanistic studies can prove difficult, phenotypic screens have enabled lead optimization, particularly by using structure-based drug design. The reader is referred to REF.<sup>127</sup> for a review on the validation of phenotypic screens of RNA targets.

### Target validation and selectivity of RNA-targeting small molecules

Direct target engagement is key to defining the MOA of a compound. Below, we describe various target validation methods based on covalent bond formation between the small molecule and the RNA target, cleavage of the RNA target and resistance profiling. Except for resistance profiling, these methods can study target engagement *in vitro*, in cells or *in vivo*.

Fortuitously, some methods not only assess engagement of the desired target but also measure selectivity. Here, we note again the difference between binding selectivity and functional selectivity. Binding selectivity, often measured *in vitro* by introducing point mutations into a model of the binding site of the small molecule, measures relative affinity and hence the extent of target occupancy. Engagement of most structures in a target RNA is biologically silent with no functional consequence. In contrast, functional selectivity measures whether target engagement has a biological effect — the function of the RNA is modulated as assessed by changes in the downstream pathways of the target and by its associated phenotype.

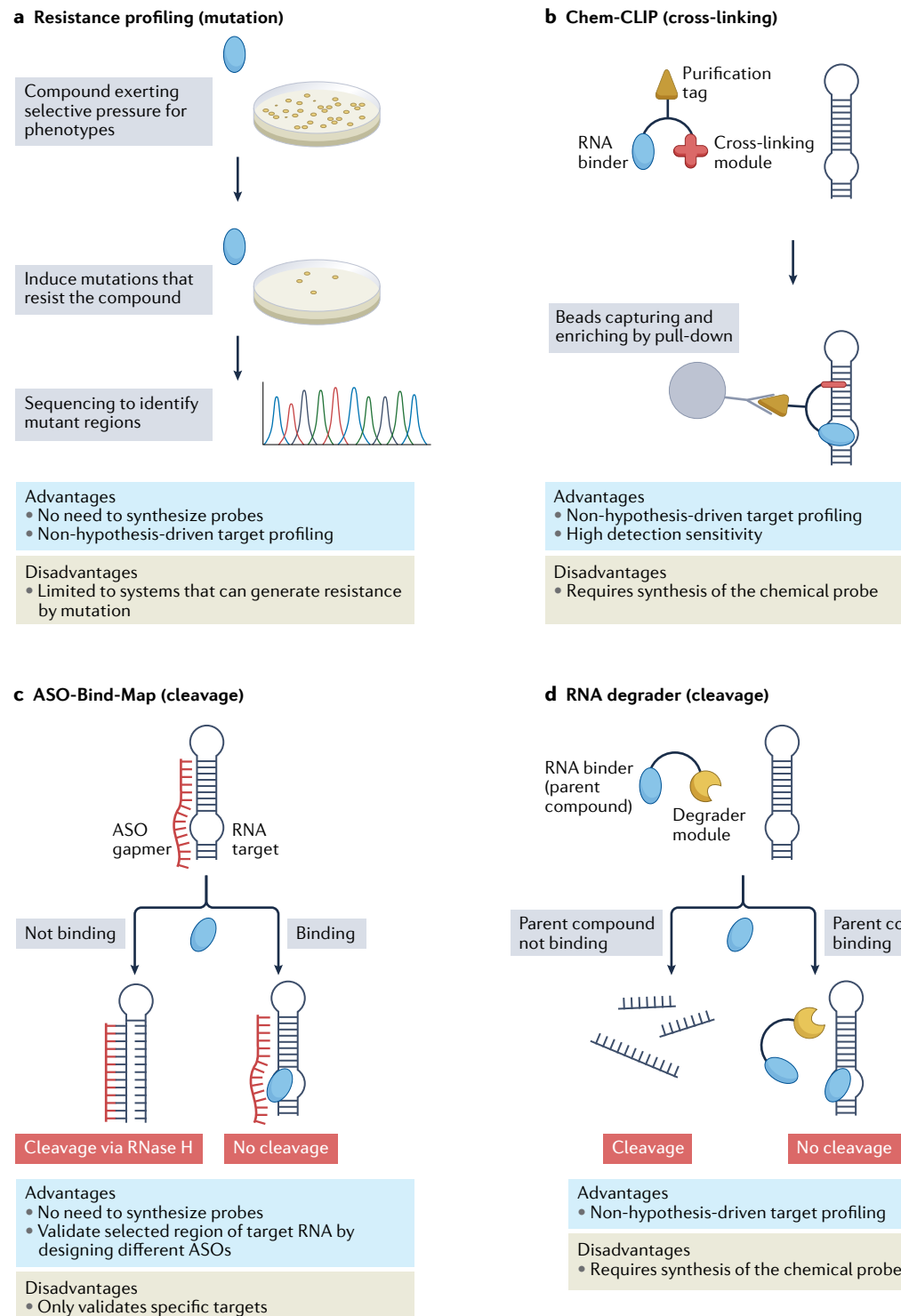
### Resistance profiling

Resistance profiling exerts selective pressure to induce mutations in bacterial or viral genomes to confer resistance (FIG. 3a). The genomes of resistant strains are sequenced to identify in which genes mutations have

---

**RNA sequencing (RNA-seq).** A high-throughput method that analyses gene expression transcriptome-wide.

**Phenotypic screening**  
A method that screens small molecules on the basis of a desired phenotypic outcome, without knowledge of its actual target.



occurred, thus identifying the target of the compound. Such an approach was used to validate the riboswitch target of ribocil (discussed below), roseoflavin and pyrithiamine<sup>11,128,129</sup> (TABLE 1). By comparison with covalent- and cleavage-based target validation methods, mutational resistance profiling does not require synthesis of chemical probes and overall has fewer experimental steps. However, it requires the small molecules to exert sufficient evolutionary pressure to induce mutational resistance, frequently used in cancer biology<sup>130</sup>.

#### Covalent bond formation to measure direct target engagement

Cellular target validation methods for RNA have been recently developed based on covalent bond formation with<sup>65,131–133</sup>, or cleavage of, the target<sup>65</sup>. One covalent method, chemical cross-linking and isolation by pull-down (Chem-CLIP; FIG. 3b), developed in 2013 (REF<sup>134</sup>), relies on functional modification of small molecules, attaching a cross-linking module (for example, diazirine or chlorambucil) and a purification handle

◀ Fig. 3 | Methods of target validation for small molecules that target RNA.

**a** | Resistance profiling is applicable when the small molecule exerts enough selective pressure to induce mutations that confer resistance. These mutations, identified by sequencing, reveal the targets of the small molecule. **b** | The target validation method Chem-CLIP (chemical cross-linking and isolation by pull-down) generates a covalent bond between a small-molecule probe and its targets, which are isolated and purified by bead pull-down. Bona fide targets are those enriched in the pulled-down fractions, as compared with the starting cell lysate. Upon co-treating increasing concentrations of the lead compound with Chem-CLIP probe, a dose-dependent restoration of the RNA target in the pulled-down fractions would indicate target engagement of the lead compound. **c** | ASO-Bind-Map is based on previous studies that show that structured regions of RNA are protected from antisense oligonucleotide (ASO) hybridization and hence ribonuclease (RNase) H degradation<sup>135,136</sup>. Thus, small molecules that bind to and stabilize the structures of RNA targets can elicit a protective effect against ASO-mediated degradation. **d** | An RNA degrader can cleave its bound RNA target either directly (bleomycin) or by recruiting endogenous RNases (RIBOTAC). Upon co-treating increasing concentrations of the lead compound with degrader probe, a dose-dependent ablation of degradation would indicate target engagement of the lead compound.

(for example, biotin or an alkyne)<sup>65</sup>. The RNA-binding module drives target engagement, bringing the cross-linking module into proximity to the RNA such that they react either directly (electrophilic in the case of chlorambucil) or upon irradiation (diazirine). Small molecule–target complexes are captured and purified with beads (streptavidin- or azide-functionalized). Quantitative PCR with reverse transcription (RT-qPCR) or RNA-seq and subsequent statistical analysis are used to analyse the enrichment of RNA targets in the pulled-down fraction, as compared with the starting lysate. Although the exact protocol may vary depending upon the chemistry of cross-linking<sup>133</sup> and purification modules, the fundamental idea of Chem-CLIP remains unchanged: transformation of dynamic reversible binding to covalent bonds by cross-linking and amplifying the signal by pull-down enrichment. Chem-CLIP experiments are completed side by side with a probe that lacks the RNA-binding module, controlling for nonspecific reaction of the cross-linking module. Indeed, this approach has validated the RNA targets of small molecules<sup>65</sup>. This method, however, requires modification of the lead compound, which can be hampered when the synthesis is challenging or if molecular recognition has not been sufficiently defined to inform a site within the small molecule not required for molecular recognition.

Chem-CLIP can also be used to study target binding and functional selectivity, when the pulled-down fractions are analysed by RNA-seq. The enrichment of a transcript indicates the extent of its occupancy by the small molecule, affording the binding selectivity of the small molecule (see ‘Quantifying selectivity’ below). Occupancy of a target RNA is not sufficient for a biological response; the small molecule must bind a functional site. Functional selectivity can be defined by comparing target occupancy with the effect on target expression by RNA-seq analysis upon treatment with the lead compound. Many RNA targets will be occupied but their expression unaffected. Pathway analysis of the RNA-seq data also provides supporting or denying evidence of on-target MOA. Identifying off-targets is key for lead optimization, and fortuitously, Chem-CLIP can identify the exact binding site within a cellular RNA, a method named Chem-CLIP-Map (REF.<sup>65</sup>).

A variant of Chem-CLIP, competitive-Chem-CLIP (C-Chem-CLIP), defines the targets of the lead compound. Briefly, cells are co-treated with a constant concentration of the Chem-CLIP probe and increasing concentrations of the lead compound. If the two molecules compete for the same binding site, a dose-dependent decrease in target enrichment should be observed as a function of lead compound concentration. C-Chem-CLIP can be used to screen other molecules for binding to the same RNA target to generate a structure–activity relationship (SAR).

#### Target cleavage to assess occupancy

Complementary cellular target validation strategies have been developed that rely on the competitive cleavage of RNA targets, including ASO-Bind-Map (FIG. 3c) and competition with RNA degraders<sup>65</sup> (FIG. 3d).

In ASO-Bind-Map, an ASO gapmer complementary to the target RNA sequence competes with a structure-binding small molecule<sup>13</sup>. In the absence of small molecule, the ASO induces cleavage by ribonuclease (RNase) H, resulting in reduced abundance of the target RNA. If a small molecule binds to the same region, it impedes hybridization of the ASO and thus diminishes target depletion. This strategy was inspired by studies that used ASOs to probe RNA folding, in which regions of RNA that fold quickly into stable structures are less accessible to ASO hybridization<sup>135,136</sup>. In contrast to Chem-CLIP, ASO-Bind-Map does not require modification of the lead compound, but does require knowledge of the binding site within the cellular RNA and that the small molecule stabilizes the structure of the RNA sufficiently to impede ASO hybridization. ASO-Bind-Map cannot be used to study selectivity transcriptome-wide, as it would require an ASO to every structure in every target. If an off-target is suspected, ASO-Bind-Map could prove or disprove target engagement.

Methods have also been developed in which the small molecule directly cleaves the RNA target or recruits a nuclease to do so, identifying both on- and off-targets by their depletion upon analysis by RNA-seq, akin to ASOs. To directly cleave RNA targets, a method dubbed small molecule nucleic acid profiling by cleavage applied to RNA (RiboSNAP), uses a lead molecule conjugated to the natural product bleomycin. Bleomycin induces strand scission of both DNA and RNA through a metal-ion and oxidative process<sup>137–142</sup>. Bleomycin A5 is typically conjugated through its terminal amine, which drives affinity for DNA; alkylation of the amine reduces DNA damage by the conjugate and directs its activity for the RNA target<sup>143</sup>. As with Chem-CLIP, side-by-side experiments are completed with a probe that lacks the RNA-binding module to control for non-selective reaction of bleomycin. The cellular targets of the small molecule–bleomycin conjugate and the control probe are identified by their depletion in RNA-seq data where bona fide targets are those cleaved only by the conjugate. Likewise, the lead compound can be studied directly in a competition experiment. As with Chem-CLIP, RiboSNAP is a robust method that can measure cellular binding selectivity by analysing the extent to which each transcript is cleaved. Functional selectivity is measured by coupling these

Structure–activity relationship (SAR). Approach that aims to correlate the chemical structure of a compound with its biological activity.

# REVIEWS

Table 1 | Examples of small molecules that bind to RNAs implicated in infectious disease

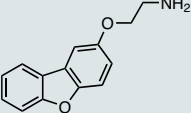
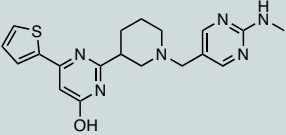
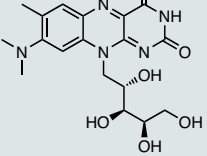
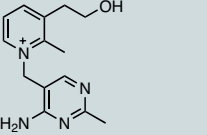
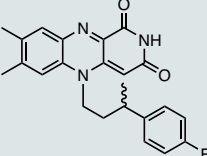
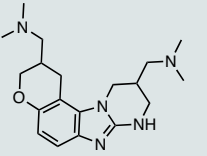
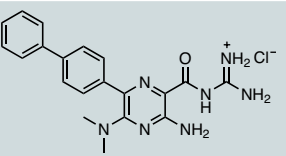
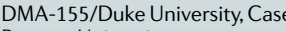
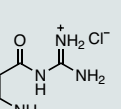
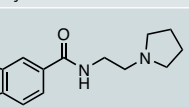
Compound/institution	Associated disease	RNA target	Mode of action	Stage of development	Activity	Refs.
	Bacterial Infection	Bacterial PreQ <sub>1</sub> riboswitch	Modulates riboswitch activity through transcriptional termination	Early discovery	$K_d = 490 \text{ nM}$ ( <i>Bs</i> aptamer domain); $K_d = 99 \text{ nM}$ ( <i>Tt</i> aptamer domain)	<sup>100</sup>
Compound 1/National Cancer Institute						
	Bacterial infection	Bacterial FMN riboswitch	Inhibits translation by binding to the FMN riboswitch	Preclinical	$K_d = 16 \text{ nM}$ ; $\text{EC}_{50} (\text{FMN reporter}) = 0.2 \mu\text{M}$	<sup>11</sup>
Ribocil/Merck						
	Bacterial infection	Bacterial FMN riboswitch	Inhibits translation by binding to the FMN riboswitch	Early discovery	$K_d = 100 \text{ nM}$	<sup>128</sup>
Roseoflavin/Yale University						
	Bacterial infection	Bacterial FMN riboswitch	Inhibits translation by binding to the FMN riboswitch	Early discovery	$K_d = 6 \mu\text{M}$ ( <i>Bacillus subtilis</i> )	<sup>129</sup>
Pyritthiamine/Yale University						
	Bacterial infection	Bacterial FMN riboswitch	Inhibits translation by binding to the FMN riboswitch	Early discovery	$K_d = 7.5 \text{ nM}$ ; $\text{MIC} = 0.5\text{--}1 \mu\text{g ml}^{-1}$ : (antibacterial activity in <i>Clostridium difficile</i> )	<sup>253,254</sup>
5FDQD/Yale University						
	Viral infection (HIV-1)	TAR apical loop	Inhibition of the Tat-TAR interaction	Early discovery	$\text{CD}_{50} = 4.4 \mu\text{M}$ (Tat/TAR-displacement FRET)	<sup>160</sup>
Amiloride/Duke University						
	Viral infection (HCV)	HCV IRES IIA domain	Inhibits translation by inducing conformational destabilization of the binding of IRES to ribosome	Early discovery	$K_d = 720 \text{ nM}$ (29-mer IIA); $\text{EC}_{50} = 5.4 \mu\text{M}$ (HCV-replicon assay)	<sup>158,180</sup>
Compound 13/University of California, San Diego						
	Viral infection (SARS-CoV-2)	5'UTR of SARS-CoV-2 RNA	Inhibits translation by perturbing the interaction between viral RNA and host protein	Early discovery	$\text{IC}_{50} = 10 \mu\text{M}$ (virus titre assay)	<sup>181</sup>
DMA-155/Duke University, Case Western Reserve University						

Table 1 (cont.) | Examples of small molecules that bind to RNAs implicated in infectious disease

Compound/institution	Associated disease	RNA target	Mode of action	Stage of development	Activity	Refs.
	Viral infection (EV71)	EV71 SLII IRES domain	Inhibits EV71 replication by stabilizing the translation repressive complex SM-SLII-AUF1	Early discovery	$K_d = 500 \text{ nM}$ (EV71 SLII RNA); $CD_{50} = 12 \mu\text{M}$ (EV71 SLII RNA by displacement)	276
DMA-135/Duke University, Case Western Reserve University						
	Fungal infection	Mitochondrial pre-rRNA group II intron	Inhibition of group II intron splicing leading to mitochondria malfunction and fungal growth inhibition	Early discovery	In vitro splicing inhibition constants ( $K_i = 0.36 \mu\text{M}$ ) MIC 2–4 $\mu\text{g ml}^{-1}$	154
Compound 19/Yale University						
	Viral infection (HIV-1)	TAR hairpin	Inhibition of the Tat-TAR interaction	Early discovery	$K_d = 49 \mu\text{M}$ (to 25-2AP TAR); $IC_{50} = 40 \mu\text{M}$ (Tat/TAR-displacement FRET)	157
Compound 15/National Cancer Institute						

$CD_{50}$ , median curative dose;  $EC_{50}$ , half maximal effective concentration; EV71, enterovirus 71; FMN, flavin mononucleotide; FRET, fluorescence resonance energy transfer; HCV, hepatitis C virus;  $IC_{50}$ , half maximal inhibitory concentration; IRES, internal ribosome entry site;  $K_d$ , dissociation constant; MIC, minimum inhibitory concentration; SARS-CoV-2, severe acute respiratory syndrome coronavirus 2; TAR, transactivation response; UTR, untranslated region.

cleavage data with the effect of the lead compound on expression levels, where indirect target expression levels are altered by the lead compound, but not depleted by the small molecule–bleomycin conjugate. RiboSNAP can also elucidate the small-molecule binding site within an RNA target.

As an alternative to direct cleavage, RNA targets can be cleaved by small-molecule chimeras that recruit a nuclelease, or ribonuclease-targeting chimeras (RIBOTACs)<sup>144</sup>. A RIBOTAC comprises an RNA-binding module tethered to an RNase L-recruiting small molecule. RNase L, which functions in the antiviral immune response, is normally expressed in minute amounts as an inactive monomer. Its activity is regulated transcriptionally, post-transcriptionally and by an RNase L inhibitor, to tightly control RNase L activity<sup>145-147</sup>. Upon viral infection, 2'-5'-oligoadenylate (2'-5'A) is synthesized, which dimerizes and activates RNase L, inducing degradation of viral RNA<sup>148,149</sup>. Previous studies have shown that RIBOTACs recruit and activate RNase L locally and do not elicit an immune response<sup>143,150</sup>. As with Chem-CLIP and direct cleavage methods, the RNA-binding molecule drives engagement of the target while a nuclease-recruiting module activates RNase L to induce cleavage; bound targets are depleted in RNA-seq analysis. To study targets engaged by the lead compound, a competition experiment can be used in which the levels of bona fide targets are restored as a function of lead compound concentration. For both direct and indirect cleavage methods, pathway analysis can be performed to evaluate on-target and potential off-target effects. An important advantage of cleavage strategies for target validation is that they do not require purification and isolation of cross-linked material; instead targets can be defined by simple RNA-seq analysis.

**Ribonuclease-targeting chimeras**  
(RIBOTACs). Small-molecule chimeras that activate and recruit endogenous ribonucleases to an RNA target to trigger its degradation.

## Gini coefficient

A statistical measurement that quantifies the selectivity of a small molecule, ranging from 0 to 1, where 0 indicates that the compound inhibits every drug target studied equally and 1 indicates a compound selective for one drug target.

## Quantifying selectivity

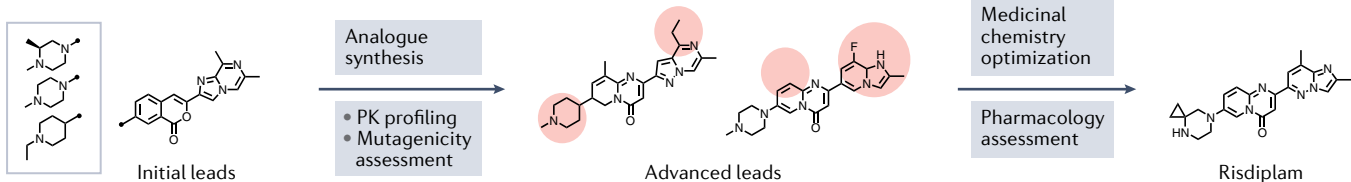
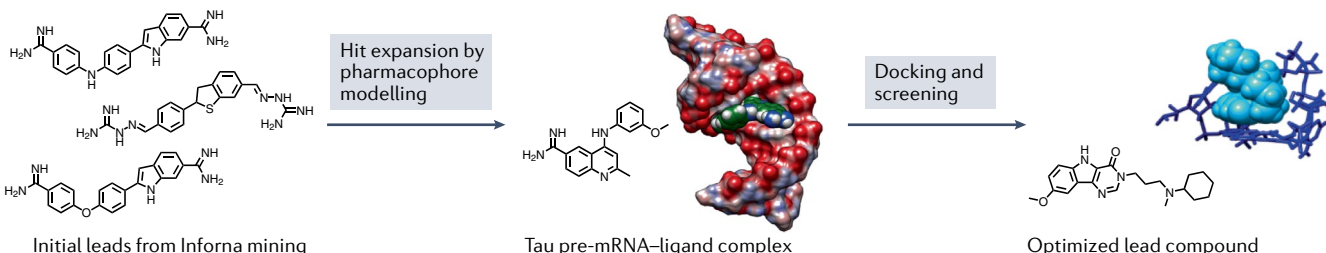
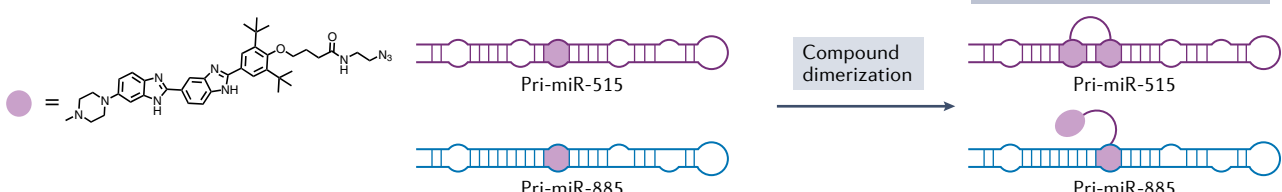
Quantifying the effect of a compound across the transcriptome, coupled with defining direct targets and pathway analysis (at the transcriptome and/or proteome level) provides insight into small-molecule selectivity. An important metric to quantify small-molecule selectivity such that small molecules can be compared is the Gini coefficient<sup>151,152</sup>. The targets of a small molecule are rank ordered by their percentage inhibition, and the cumulative fraction and the total cumulative effect for each are calculated. The former is a function of the number of targets studied and the latter is a weighted inhibition. The two values are plotted against each other, and the Gini coefficient is equal to  $1 - 2B$  where  $B$  is the area under the resulting curve<sup>153</sup>. For a review of Gini coefficients as applied to RNA, the reader is referred to REF.<sup>152</sup>.

## **Lead optimization of RNA-targeting small molecules**

One advantage of small-molecule therapeutics is that medicinal chemistry efforts can be applied to optimize the initial hit compound, improving both its potency and its physicochemical properties. Below, three broad strategies to lead-optimize RNA-targeting small molecules — including traditional medicinal chemistry as well as structure-guided and modular assembly approaches, which are often integrated synergistically — are discussed.

## **Traditional medicinal chemistry approaches**

Traditional medicinal chemistry optimization typically starts with analogue synthesis or purchase to establish the SAR around the hit compound (FIG. 4a). The bioactivity of an RNA-targeting ligand can be affected by

**a Traditional medicinal lead optimization****b Structure-guided lead optimization****c Sequence-based lead optimization**

**Fig. 4 | Strategies for lead optimization of RNA-targeted small molecules.** **a** | Traditional medicinal chemistry optimization begins with hit expansion and analogue synthesis to generate structure–activity relationships (SARs), which can be used to optimize lead compounds as well as to discover new scaffolds by pharmacophore modelling. **b** | Structure-guided lead optimization relies on structure modelling of the RNA target to perform virtual screening and to inform compound design based on ligand–RNA interactions. **c** | Sequence-based lead optimization explores the differences between structures of on-target and off-targets and modifies the lead compound based on structural features unique to the on-target, that is, modular assembly or dimerization. PK, pharmacokinetic; pri, primary.

multiple factors, such as binding affinity, cellular permeability and the number of off-targets. SAR is typically defined by a combination of biophysical and cellular assays to evaluate hit analogues. After acquiring sufficient SAR data, pharmacophore modelling and subsequent chemical similarity searching can then diversify and optimize the starting scaffold. Among all scaffolds, those with desirable or optimizable physicochemical properties are prioritized. Traditional medicinal chemistry can be applied to essentially any small-molecule candidate, tempered by the resources required to synthesize or purchase a large number of analogues. Below, we describe how medicinal chemistry approaches were used to optimize risdiplam, a treatment for SMA, and a pyrimido-indole that directs *MAPT* alternative splicing. The reader is referred to REFS. <sup>154–159</sup> for other notable examples of lead optimization of RNA-targeted small molecules using medicinal chemistry.

**Structure-guided approaches**

Structure-guided approaches for lead optimization rely on sophisticated models of a ligand–RNA complex to define key interactions and identify how positions within the compound's structure can be modified to improve

interactions or eliminate those that are unfavourable (FIG. 4b). Such models are typically experimentally generated by NMR spectroscopy or X-ray crystallography. The dynamic nature of RNA must be considered, as no single static structure can truly represent all possible conformations. To address this limitation, experimental models are often coupled with molecular dynamics simulations to generate an ensemble of structures, where the algorithm simulates RNA conformations on the basis of experimentally determined parameters.

Molecular dynamics-based virtual screening has successfully identified ligands that bind various RNAs, typically using models from NMR spectroscopy or X-ray crystallography. As these structures do not capture the dynamic nature of RNA, and molecular dynamics simulations do not accurately recapitulate RNA electrostatics, docking of small-molecule ligands is not as predictive as it could be. To overcome these challenges, a docking method that uses the dynamic ensemble of RNA conformations from combined NMR and molecular dynamics approaches has been developed, an example of which is provided below<sup>126,160</sup>. The advantage of structure-based approaches is that they minimize the synthesis efforts by rationally designing analogues,

but the limitation is that not all target structures are readily attainable.

### Modular assembly approaches

One of the many factors that affect the activity of small molecules that target RNA is the uniqueness of the structural motif throughout the transcriptome. A strategy to optimize small molecules with activity against degenerate functional structures is to exploit adjacent structural elements, that is, a modular assembly approach in which a single small molecule binds to structural elements that are uniquely juxtaposed (FIG. 4c). Indeed, polyvalency — used in various biological processes to enhance avidity and specificity, from cell–cell interactions to gene expression and viral infections — has also been exploited in drug discovery efforts to agonize or antagonize receptors<sup>161,162</sup>. Such an approach has been taken for RNA targets by modularly assembling two or more RNA-binding modules<sup>65,163–166</sup>, some with *in vivo* activity<sup>167</sup>. One example is described below in which a modular assembly approach broke the degeneracy of two motifs, affording a specific inhibitor of miR-515 biogenesis. Modular assembly has been employed for RNA repeat expansions (BOX 2), which display periodic arrays of internal loops.

### Box 2 | Modular assembly strategy for targeting RNA repeat expansions

RNA repeat expansions are perhaps ideal targets for a modular assembly strategy. Known to cause more than 40 neurodegenerative and neuromuscular diseases<sup>287,288</sup>, expanded repeats often adopt a hairpin structure with a periodic array of internal loops. Toxicity is initiated when an RNA repeat expansion reaches a length that corresponds to a shift in structure<sup>59,289</sup>. Selective recognition of RNA repeat expansions is possible by exploiting the structural differences between the toxic repeats and short non-pathogenic repeats — differences that have been both experimentally and computationally validated<sup>59,278,289–291</sup>.

Selectivity can also be derived from the effective concentration of the toxic structure. Most expansions have hundreds to thousands of repeats. The effective concentration of the disease-causing structural element is therefore much greater than the concentration of the RNA in which it is embedded and in many potential off-targets. Small molecules are therefore more likely to encounter and engage the toxic repeat and affect its biology selectively. Further, repeats may be particularly sensitive to small-molecule intervention despite their size. For RNA gain-of-function pathology, freeing just a fraction of sequestered protein can improve disease-associated defects<sup>292</sup>.

Many laboratories have developed dimers that target two internal loops formed by repeat expansions, including those that cause myotonic dystrophy type 1 (DM1)<sup>163,293</sup> and type 2 (DM2)<sup>294</sup>, c9orf72–amyotrophic lateral sclerosis (ALS)/frontotemporal dementia (FTD)<sup>295</sup> and so on, although some have mixed MOAs as they also inhibit transcription. In one interesting example with an RNA-centric MOA, a dimer that targets r(CUG)<sup>exp</sup> was functionalized with azide and alkyne handles<sup>293</sup>. Upon binding to adjacent sites in the RNA target in patient-derived cells, a proximity-based click reaction afforded higher order oligomers that were formed in cells, that is, an on-site probe synthesis approach that increased potency from the nanomolar range to the picomolar range<sup>293</sup>. Further, this strategy enabled imaging of the repeats in live, patient-derived cells<sup>293</sup>. Such an approach was later extended to a tetrazine ligation reaction<sup>296</sup>.

Modularly assembled small molecules that bind r(CUG) repeat expansions have also been conjugated to bleomycin A5 (Cugamycin; TABLE 3) to cleave the RNA target selectively in myotubes derived from patients with DM1 and in a mouse model<sup>278</sup>. Importantly, Cugamycin alleviated DM1-associated defects without inducing DNA damage or lung fibrosis, known side effects of bleomycin<sup>137,297</sup>. (Please see ‘Target cleavage to assess occupancy’ section for more details about small molecule–bleomycin conjugates.) *In vivo*, Cugamycin rescued 97% of DM1-associated splicing defects, expression of the muscle-specific chloride ion channel and myotonia, with no significant off-targets. Additionally, small molecule–bleomycin conjugates have been developed for other targets including oncogenic pri-miR-96 (REFS. 167,298) and the miR-17/92 cluster<sup>299</sup> as well as r(CCUG)<sup>exp</sup> in intron 1 of CNBP, which causes DM2 (REF. 300).

### Examples of small-molecule RNA binders

Several examples in which small-molecule RNA binders perturb downstream biology in a precise and predicted manner are highlighted below. Notably, the small molecules directly engage a functional site, and simple binding is sufficient to exert a biological effect (BOX 1 and TABLES 1–3).

### Targeting functional RNA structures

Many RNA classes have functional sites, for example, Drosha and Dicer processing sites within miRNA precursors, IRESs in viral RNAs and some human mRNAs, bacterial riboswitches, splicing enhancers and silencers in pre-mRNAs, and regulatory structures in 5' and 3' untranslated regions (UTRs). Below, we describe the discovery of exemplar small molecules that bind to these functional sites.

**Discovery of small molecules that bind viral RNAs.** Apart from the bacterial ribosome, noncoding regions have also been investigated as drug targets to treat viral infections such as those caused by HIV<sup>160,168</sup> and hepatitis C virus (HCV)<sup>12</sup>. The first viral regulatory elements targeted by small molecules that interfere with the infection process were HIV TAR and RRE RNAs<sup>169–174</sup>. Structure-guided approaches have been used to identify new scaffolds for TAR RNA that inhibited Tat-mediated transcriptional activation in a cellular model. One such scaffold, amiloride (TABLE 1), was later lead-optimized, affording an analogue with >100-fold enhanced affinity compared with the entry compound, and its structural interactions with the RNA target were well characterized<sup>126,160</sup>.

The HCV mRNA harbours a highly structured and conserved IRES in its 5'UTR, which initiates translation by recruiting and assembling host ribosomes<sup>175–177</sup> and can be inhibited by small-molecule binding<sup>67,178,179</sup>. A mass spectrometry-based screen identified 2-aminobenzimidazole derivatives as both binders and inhibitors of HCV translation (TABLE 1). The affinity of the lead scaffold was improved ~100-fold after SAR studies<sup>158,180</sup>.

Another amiloride was discovered that inhibits viral replication of the *Betacornoavirus* OC43 and SARS-CoV-2 (REF. 181). A panel of 23 amilorides was screened for inhibition of the infectivity of OC43, affording three lead molecules. Sequence conservation of the 5'-end of betacoronaviruses suggested a functional role, and this region is predicted to fold into six stem-loop structures (SL1–SL6). Fortunately, one amiloride bound to SL6, as determined by a dye displacement assay and NMR spectral studies<sup>181</sup>.

**Discovery of an antifungal that targets a group II intron.** Group II introns are a class of self-splicing ribozymes found in mitochondria of fungi and yeast but not in mammals<sup>182</sup>, making them perhaps ideal targets for the development of antifungals. An *in vitro* screen of ~10,000 compounds for inhibitors of group II intron splicing afforded six hits that served as starting points<sup>154</sup>. Pharmacophore analysis enabled by SAR studies provided alternative scaffolds with improved physicochemical properties and ultimately a low micromolar

Table 2 | Examples of small molecules that bind to RNAs implicated in cancer

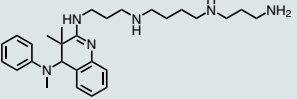
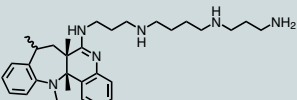
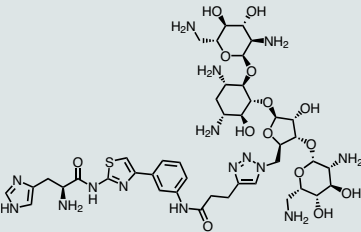
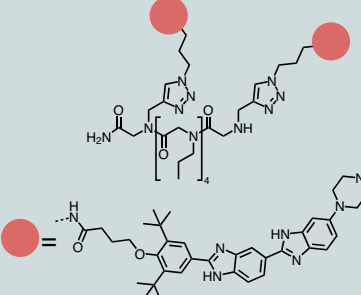
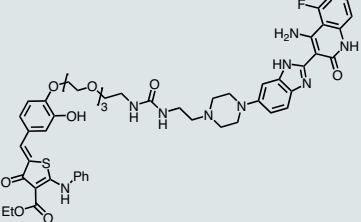
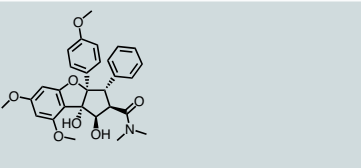
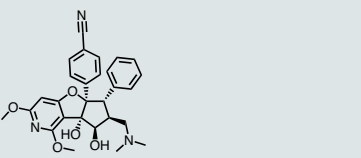
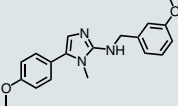
Compound/institution	Associated disease	RNA target	Mode of action	Stage of development	Activity	Ref.
	Gastric carcinoma	Pre-miR-372	Inhibits Dicer processing	Early discovery	$K_d = 150 \text{ nM}$ ; $IC_{50}(\text{Dicer cleavage}) = 1.06 \mu\text{M}$ , $IC_{50} = 20 \mu\text{M}$	<sup>192</sup>
PA-1/Université Côte d'Azur						
	Gastric carcinoma	Pre-miR-372	Inhibits Dicer processing	Early discovery	$K_d = 110 \text{ nM}$ ; $IC_{50}(\text{Dicer cleavage}) = 0.58 \mu\text{M}$	<sup>16</sup>
PA-2/Université Côte d'Azur						
	Breast cancer	Pre-miR-21	Inhibits Dicer processing	Early discovery	$K_d = 50.7 \text{ nM}$ ; $IC_{50}(\text{Dicer cleavage}) = 1.55 \mu\text{M}$	<sup>193</sup>
Neomycin-nucleobase-amino acid conjugate (compound 6b)/Université Côte d'Azur						
	Breast cancer	Pre-miR-515	Dimeric compound that targets Drosha processing site and adjacent site for enhanced selectivity	Early discovery	$K_d = 60 \text{ nM}$ ; $IC_{50} = 0.2 \mu\text{M}$ (MCF-7 cells)	<sup>194</sup>
Targaprimir-515/Scripps Research Institute						
	Triple-negative breast cancer and Alport syndrome	Pre-miR-21	Induces degradation of miR-21 via RNase L recruitment	Early discovery	$K_d = 3 \mu\text{M}$ (A bulge 3 $\times$ 2 RNA ILL); reduced levels of miR-21 by ~31% at 0.2 $\mu\text{M}$	<sup>150</sup>
Dovitinib-RIBOTAC/Scripps Research Institute						
	Leukaemia	Polypurine sequences in the 5'UTR of a subset of oncogenic mRNAs	Inhibits translation initiation by clamping eIF4A to polypurine RNA sequence in the 5'UTR	Early discovery	$K_d = 26 \text{ nM}$ (ternary complex between compound, r(AG) <sub>10</sub> and eIF4A)	<sup>265</sup>
Rocaglamide/UC Berkeley & RIKEN						
	Triple-negative breast cancer and chronic myelogenous leukaemia	Polypurine sequences in the 5'UTR of a subset of oncogenic mRNAs	Inhibits translation initiation by clamping eIF4A to polypurine RNA sequence in the 5'UTR	Phase I-II clinical trial: NCT04092673	$K_d = 21-69 \text{ nM}$ (ternary complex between compound, r(AG) <sub>3</sub> and eIF4A); $IC_{50} = 10.06 \text{ nM}$ (MDA-MB-231 cell proliferation)	<sup>266</sup>
Zotentifin (eFT226)/eFFECTOR Therapeutics & Inception Therapeutics						

Table 2 (cont.) | Examples of small molecules that bind to RNAs implicated in cancer

Compound/institution	Associated disease	RNA target	Mode of action	Stage of development	Activity	Ref.
	Breast cancer	MALAT1	Binds and modulates element for nuclear expression (ENE) triplex	Early discovery	$K_d = 2.3 \mu\text{M}$ ; $\text{IC}_{50}$ about $1 \mu\text{M}$ (RNA level in MMTV-PyMT tumours)	97

Compound 5/National Cancer Institute

$\text{EC}_{50}$ , half maximal effective concentration; eIF4A, eukaryotic initiation factor 4A;  $\text{IC}_{50}$ , half maximal inhibitory concentration;  $K_d$ , dissociation constant; miR, microRNA; MMTV-PyMT, mouse mammary tumour virus polyoma middle tumour antigen; RNase, ribonuclease; UTR, untranslated region.

inhibitor of group II intron splicing with antifungal activity comparable to that of amphotericin B.

**Targeting human miRNAs with small molecules.** miRNAs, small noncoding RNAs of 20–25 nucleotides, are key players in post-transcriptional gene regulation, silencing gene expression by association with the Argonaute RNA-induced silencing complex (RISC) and base pairing to the 3'UTR of complementary mRNAs<sup>8,183,184</sup>. Transcribed by RNA polymerase II as primary transcripts (pri-miRNAs), they are processed stepwise, first by the nuclease Drosha into precursor miRNAs (pre-miRNAs); after export to the cytoplasm, the mature (functional) miRNA is generated by the nuclease Dicer<sup>149,185</sup>. Fortunately, their structures can be accurately modelled from sequence, and processing (functional) sites can be deduced from deep sequencing of mature miRNAs. Many studies have shown that Drosha or Dicer processing sites within miRNA precursors are targetable functional structures that can be short-circuited to alleviate disease<sup>159,167,186–190</sup>.

Compounds that bind functional structures in miRNA precursors and selectively inhibit the biogenesis of oncogenic miRNAs have been identified<sup>191</sup>. In particular, a spermine-amidine conjugate (PA-1) was discovered using an assay that measures enzymatic inhibition of pre-miR-372 processing<sup>192</sup> (FIG. 5a and TABLE 2). In vitro, the molecule, without optimization, bound to the pre-miR-372 Dicer site, inhibited its processing and reduced cancer cell proliferation by derepression of its downstream target large tumour suppressor kinase 2 (*LATS2*)<sup>192</sup>. The selectivity of the small molecule was studied miRNome-wide, which revealed that only a small subset of miRNAs were affected. The conjugate also reduced formation of tumour cell spheroids of patient-derived cancer stem cells<sup>192</sup>. PA-1 was later optimized to afford the pre-miR-372-selective small molecule PA-3 (REF. <sup>16</sup>) (TABLE 2). Interestingly, a neomycin-nucleobase-amino acid conjugate that inhibited pre-miR-372 and pre-miR-21 was discovered by the same laboratory; lead optimization by structure-based design afforded a selective inhibitor of pre-miR-21 (REF. <sup>193</sup>) (TABLE 2).

Modular assembly has been used to overcome the degeneracy of functional RNA structures in the transcriptome by targeting two adjacent structures in the RNA target with a single molecule. Such an approach was taken to distinguish between human pri-miR-515 and pri-miR-885 to afford a selective molecule that inhibits only the biogenesis of miR-515 (REF. <sup>194</sup>) (FIG. 4a and TABLE 2).

The lead molecule, a *bis*-benzimidazole with steric bulk that ablates DNA binding, prefers a structure harboured in the Drosha processing sites of both pri-miR-885 and pri-miR-515, a 5'UCU/3'AUA internal loop. As expected, the compound inhibited the biogenesis of both miRNAs to a similar extent in cells. To drive the selectivity towards a single target, differences in the secondary structure of the two pri-miRNAs were identified and exploited. A second internal loop that binds the substituted *bis*-benzimidazole is present adjacent to the Drosha site of miR-515, but not that of miR-885. Therefore, a dimeric compound, dubbed Targaprimir-515, consisting of two copies of the original hit, was designed. By comparison with the monomeric ligand, which showed similar affinity for both RNA targets, Targaprimir-515 had no measurable binding to RNA with a singular binding site and 3,200-fold improvement in affinity to pri-miR-515 (REF. <sup>194</sup>). The enhancement of selectivity in cells was also evident by miRNA profiling and global proteomics. The self-structure of Targaprimir-515 contributed to the improved in vitro and cellular selectivity<sup>194</sup>. Collectively, these and other studies<sup>65</sup> confirm that bivalent compounds, even those assembled from fragments<sup>108</sup>, can successfully target RNAs with greater affinity and selectivity than the monomer from which they are derived. Modular assembly has also been applied to target RNA repeat expansions with enhanced potency and specificity (BOX 2).

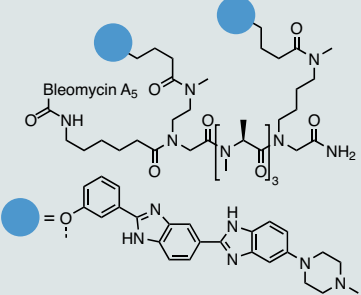
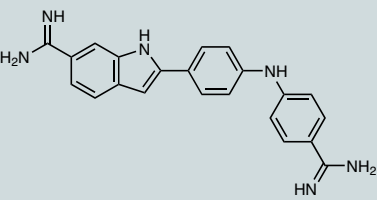
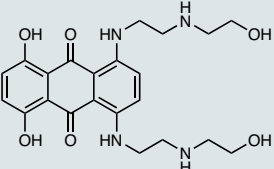
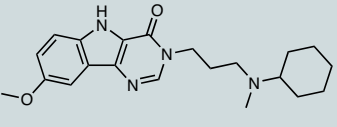
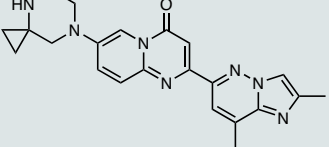
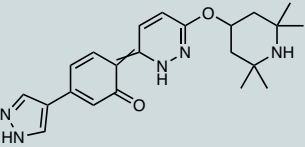
**Inhibiting undruggable proteins by targeting the encoding RNA:  $\alpha$ -synuclein.** Pathogenic proteins are often considered undruggable when they lack a defined structure<sup>195,196</sup>. One way to drug these intrinsically disordered proteins (IDPs) is to inhibit their translation by targeting the encoding mRNA. Iron-responsive elements (IREs) are small stem-loop structures present in 5'- or 3'UTRs<sup>197–199</sup> that bind to iron regulatory proteins (IRPs)<sup>200,201</sup>. IRP binding to IREs in the 5'UTR prevents ribosome docking and blocks RNA translation whereas binding to the 3'UTR stabilizes the transcript and upregulates translation<sup>202</sup>. IREs have an important role in cognitive function and hence in neurodegenerative diseases<sup>203–207</sup>. Small molecules that target IREs and inhibit the translation of these pathogenic proteins have been discovered<sup>13,197,208–213</sup>.

The aberrant expression and mutation of the IDP  $\alpha$ -synuclein, which harbours an IRE in the encoding SNCA mRNA, is linked to Parkinson disease<sup>214,215</sup>. Targeting the IRE in the SNCA mRNA with small molecules to inhibit its translation is thus a promising

Intrinsically disordered proteins (IDPs). Proteins that lack well-defined 3D structures and are thus considered undruggable.

**Iron-responsive elements (IREs).** Small stem-loop structures present in 5' or 3' untranslated regions (UTRs) that bind to iron regulatory proteins (IRPs). IRP binding to IREs in the 5'UTR prevents ribosome docking and blocks RNA translation whereas binding to the 3'UTR stabilizes the transcript and upregulates translation.

Table 3 | Examples of small molecules that bind to RNAs implicated in neuromuscular and neurodegenerative diseases

Compound/institution	Associated disease	RNA target	Mode of action	Stage of development	Activity	Refs.
	Myotonic dystrophy type 1	r(CUG) <sup>exp</sup> in DMPK mRNA	Displaces MBNL1 from binding to r(CUG) <sup>exp</sup>	Early discovery	$K_d = 365 \text{ nM}$ (for r(CUG) <sub>12</sub> ); $EC_{25} = 840 \text{ nM}$ (rescued splicing defects)	<sup>278</sup>
Cugamycin/Scripps Research Institute						
	Parkinson disease	Iron-responsive element in α-synuclein mRNA	Inhibits ribosomal assembly and polysome loading onto α-synuclein mRNA	Early discovery	$K_d = 1.5 \mu\text{M}$ ; $IC_{50}$ (neurons) = $0.5 \mu\text{M}$	<sup>13</sup>
Synucleozid/Scripps Research Institute						
	Alzheimer disease; frontotemporal dementia with parkinsonism-17	Exon 10-intron junction in MAPT pre-mRNA	Inhibits binding of splicing machinery at the exon 10-intron junction; also inhibits a fungal group II intron <sup>277</sup>	Early discovery	$K_d < 1 \mu\text{M}$ ; $EC_{50} = 700 \text{ nM}$ (competition of binding with 25 nM pyrene-neomycin conjugate)	<sup>225,279</sup>
Mitoxantrone/University of Washington, Seattle						
	Alzheimer disease; frontotemporal dementia with parkinsonism-17	Exon 10-intron junction in MAPT pre-mRNA	Inhibits binding of splicing machinery at the exon 10-intron junction	Early discovery	$K_d = 4.9 \mu\text{M}$ ; $IC_{50}$ (transfected HeLa cells) = $10 \mu\text{M}$ ; decreased 4R/3R ratio by ~50% in primary neurons at $40 \mu\text{M}$	<sup>70,228</sup>
Compound 9/Scripps Research Institute						
	SMA	SMN2 pre-mRNA exon 7-intron junction	Promotes exon inclusion by stabilizing the binding of the splicing machinery	FDA approved	$K_d = 15 \text{ nM}$ ; $EC_{1.5x}$ (SMA patient-derived fibroblasts) = $7 \text{ nM}$	<sup>14</sup>
Risdiplam/Roche and PTC Therapeutics						
	SMA; HD	SMN2 pre-mRNA exon 7-intron junction	Promotes exon inclusion by stabilizing the binding of the splicing machinery	Phase I/II clinical trial (for SMA: NCT02268552; for HD: NCT05111249)	$EC_{50}$ (SMN ELISA in SMNΔ7 mouse myoblasts) = $20 \text{ nM}$	<sup>15</sup>
Branaplam						

$EC_{50}$ , half maximal effective concentration; ELISA, enzyme-linked immunosorbent assay; HD, Huntington disease;  $IC_{50}$ , half maximal inhibitory concentration;  $K_d$ , dissociation constant; SMA, spinal muscular atrophy; SMN, survival of motor neuron.

strategy<sup>216</sup>. Synucleozid, a small molecule that binds a bulged adenosine residue within the IRE structure and inhibits SNCA translation, was designed by Infora<sup>13</sup> (FIG. 5b and TABLE 3). Notably, this bulged adenosine is

not present in other IREs. Recognition of the SNCA IRE by synucleozid was dependent upon both the bulged nucleotide and its closing base pairs<sup>13</sup>; its MOA, by direct target engagement, was reduction of the number of

polysomes loaded onto SNCA mRNA. Approximately 90 mRNAs have been identified with IREs or IRE-like elements, which vary in their sequences and structures<sup>199</sup>; these studies and those mentioned above lay the foundation for regulating translation of other mRNAs with small molecules.

**Altering protein isoforms by directing exon exclusion with small molecules: microtubule-associated protein tau.** Almost every pre-mRNA goes through a series of processing steps, including alternative splicing (inclusion or exclusion of exons) to produce different protein isoforms<sup>217</sup>. Unsurprisingly, splice site mutations can

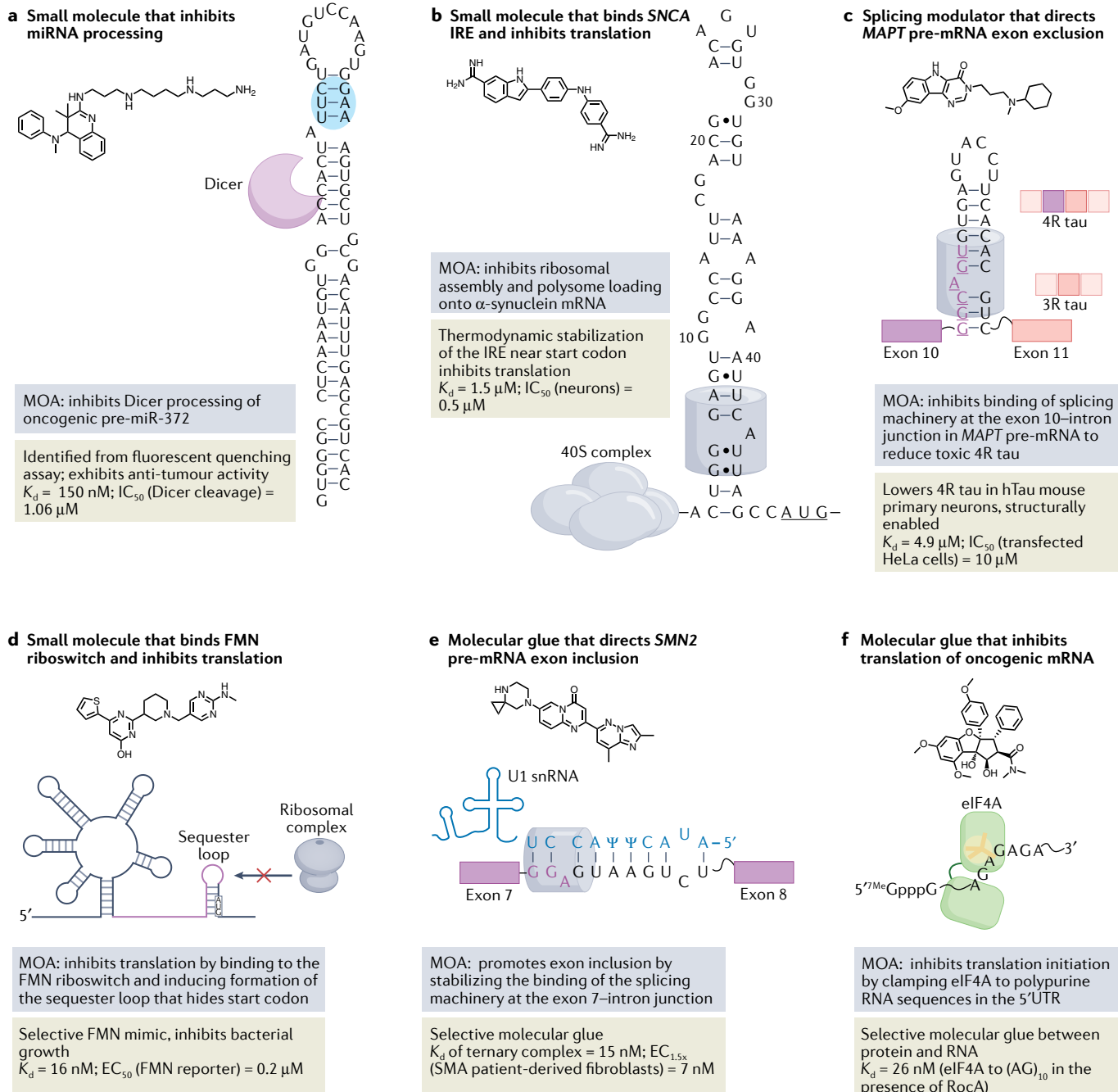


**Fig. 5 | Small-molecule binding to RNA structures elicits biological effects through various modes of action.** **a** | A small molecule that binds the Dicer site of oncogenic pre-miR-372 inhibits its biogenesis and short-circuits downstream pathways. **b** | A compound that binds to an iron-responsive element (IRE) in the 5' untranslated region (UTR) of SNCA mRNA inhibits its translation by mechanically blocking ribosomal assembly and polysome loading onto the mRNA. **c** | A small molecule that binds to a structural element at the exon 10–intron junction of MAPT pre-mRNA directs alternative splicing towards exon exclusion, reducing the amount of toxic 4R tau produced. **d** | A small molecule inhibits translation by binding to the flavin mononucleotide (FMN) riboswitch and inducing formation of the sequester loop that hides the start codon. **e** | Another small molecule, later optimized into an FDA-approved drug for the treatment of spinal muscular atrophy, binds to the exon 7–intron junction in SMN2 pre-mRNA and increases SMN2 protein levels by acting as a molecular glue for the RNA and splicing machinery and promoting exon inclusion. **f** | A compound binds to polyuridine sequences in 5'UTRs of a subset of mRNAs and inhibits translation by acting as a molecular glue for the RNA and eukaryotic initiation factor 4A (eIF4A).  $\text{IC}_{50}$ , half maximal inhibitory concentration;  $K_d$ , dissociation constant; miR, microRNA; MOA, mode of action.

the flavin mononucleotide (FMN) riboswitch and inducing formation of the sequester loop that hides the start codon. **e** | Another small molecule, later optimized into an FDA-approved drug for the treatment of spinal muscular atrophy, binds to the exon 7–intron junction in SMN2 pre-mRNA and increases SMN2 protein levels by acting as a molecular glue for the RNA and splicing machinery and promoting exon inclusion. **f** | A compound binds to polyuridine sequences in 5'UTRs of a subset of mRNAs and inhibits translation by acting as a molecular glue for the RNA and eukaryotic initiation factor 4A (eIF4A).  $\text{IC}_{50}$ , half maximal inhibitory concentration;  $K_d$ , dissociation constant; miR, microRNA; MOA, mode of action.

alter splicing patterns and cause human diseases<sup>218</sup>. Studies with oligonucleotides demonstrated that it is indeed possible to rescue splicing defects by binding to and occluding the mutation from the spliceosomal machinery<sup>60,219–222</sup>, suggesting that small molecules may also be able to direct splicing.

The microtubule-associated protein tau gene (*MAPT*) produces six tau isoforms by alternative splicing<sup>223</sup>. Exons 9–12 encode a microtubule-binding domain (MBD), and exon 10 is alternatively spliced to produce isoforms with three (3R) or four (4R) MBDs, with the latter prone to aggregation<sup>223</sup>. In healthy individuals, the ratio between 3R and 4R is approximately equal; however, a genetic mutation in the splicing regulatory element (SRE) present in exon 10 alters the splicing pattern to produce excess 4R, the cause of frontotemporal dementia with parkinsonism-17 (FTDP-17). One such intronic mutation, dubbed disinhibition dementia parkinsonism amyotrophy complex (DDPAC), converts a GC base pair into a GU wobble pair, destabilizing the structure of the SRE. This destabilization allows U1 small nuclear RNA (snRNA) to more easily bind the SRE and facilitate exon 10 inclusion<sup>224</sup>. Stabilization of the structure of the SRE with a small molecule might therefore impede U1 snRNA binding and restore a normal splicing pattern. Various small molecules have been identified that bind to the SRE<sup>70,225–228</sup> (FIG. 5c and TABLE 3).

Small molecules with activity in primary neurons were lead-optimized by chemical similarity searching, pharmacophore modelling driven by *in vitro* and cellular screening and analogue synthesis, structure-based design and docking studies based on the 3D structure of the *MAPT* SRE bound to several lead molecules, and traditional medicinal chemistry approaches<sup>70</sup> (FIG. 4b). This synergistic strategy afforded a drug-like molecule that directed *MAPT* splicing towards the 3R isoform in primary neurons from a human tau transgenic mouse<sup>70</sup>.

#### Targeting RNA structures for degradation

If a functional site has not yet been discovered, various strategies may be applied to modulate RNA function by facilitating its degradation (FIG. 6). Two of these strategies are discussed below; both rely on chemically induced proximity — direct small-molecule cleavage of the target RNA (BOX 2) or target degradation achieved by nuclease recruitment (FIG. 6a). Although these examples target known functional structures, the cleavage-based methods eliminate the RNA transcript and thus their MOA does not require binding to a functional site. The advantage of small molecule degraders, like ASOs, is that they are simultaneously target-validation methods. Small molecules can also facilitate degradation of an RNA target by increasing its accessibility to endogenous decay pathways such as the exosome and directing splicing such that the mature mRNA encodes a premature stop codon (FIG. 6b).

**Nuclease recruitment to cleave RNA targets: ribonuclease-targeting chimeras.** Targeted degradation was first demonstrated for proteins, or proteolysis-targeting chimeras (PROTACs)<sup>229</sup>. PROTACs are chimeric molecules comprising a protein-binding module and an

E3 ubiquitin ligase-recognition module, which tags the targeted protein for selective degradation by the proteasome<sup>230–234</sup>. RIBOTACs have been developed for targeted degradation of RNA<sup>144</sup>, composed of an RNA-binding module and a RNase-recruiting module that selectively mediates RNA decay (FIG. 6a). RIBOTACs recruit the ubiquitously expressed cellular endoribonuclease RNase L, which functions in the viral immune response (see above)<sup>148,149</sup>. In its first two iterations, an RNA-binding module that selectively recognizes the Drossha site of pri-miR-96 or the Dicer site of pre-miR-210 was coupled to 2'-5'A<sub>4</sub> inducing its selective cleavage in cells<sup>144,235</sup>.

As 2'-5'A<sub>4</sub> reduces drug-likeness, a small-molecule RNase L recruiter was developed<sup>143</sup> based on a previously reported small molecule<sup>236</sup>. A RIBOTAC with this new recruiter was developed to target pre-miR-21 for degradation by recognition of its Dicer processing site<sup>143</sup>. Notably, the RIBOTAC was more potent than the binder from which it was derived, possessed a prolonged duration of effect and inhibited breast cancer metastasis in a mouse model. Transcriptome-wide studies showed that the RIBOTAC was also more selective than the binder<sup>143</sup>, as quantified by a Gini coefficient<sup>153</sup> and did not elicit an immune response. This enhanced selectivity is a composite of the specificity of the RNA-binding small molecule, the inherent substrate specificity of RNase L and whether the target has an RNase L substrate adjacent to the site at which the RNA-binding small molecule binds, the distance dictated by the linker that tethers the two components of the chimera.

These studies led to the hypothesis that RIBOTACs may allow reprogramming of known drugs for RNA targets. 2DCS selection of the Repurposing, Focused Rescue, and Accelerated Medchem (ReFRAME) library<sup>237</sup> indicated that the receptor tyrosine kinase (RTK) inhibitor dovitinib binds the Dicer processing site of pre-miR-21 and therefore might inhibit its cellular processing, albeit at higher concentrations than those required to inhibit RTKs<sup>150</sup>. Converting the binding molecule dovitinib into a RIBOTAC enhanced its inherent RNA-targeting activity in cells and concomitantly decreased potency against canonical RTK protein targets, shifting selectivity for pre-miR-21 by 2,500-fold (TABLE 2). Further, the chimera alleviated disease progression in two mouse models caused by miR-21 overexpression: triple-negative breast cancer and Alport syndrome<sup>150</sup>.

RNA function can indeed be modulated with small-molecule binders or small-molecule degraders, expanding the MOA of RNA-targeting compounds and likely the number of targetable RNAs. Chimeric small molecules that target RNAs set the foundation for new drug discoveries akin to the revolution of PROTACs, enabling inhibition of RNA circuits when the functional site is unknown or absent. It will be exciting to see whether other RNA-modifying enzymes (editing, splicing machinery and so on) can be selectively recruited to RNA targets.

#### Targeting RNA-associated pathways

Several small molecules that target RNA-associated pathways have been derived from phenotypic screening and are described below.

**Proteolysis-targeting chimeras**  
(PROTACs). Chimeric molecules comprising a protein-binding module and a E3 ubiquitin ligase-recognition module, which tags the targeted protein for selective degradation by the proteasome.

**Ribocil, an antibacterial that targets the FMN riboswitch.** Riboswitches are structured noncoding sequences in the 5' leader of bacterial mRNAs that control gene expression of a downstream ORF<sup>61,238–242</sup> (FIG. 5d). Widely distributed across all known phylogenetic groups of bacteria, riboswitches form highly specific binding pockets for small-molecule metabolites, second messengers and inorganic ions<sup>243–247</sup>. Binding of the small molecule to the receptor (aptamer) domain

directs formation of alternative secondary structures in the adjacent regulatory domain (expression platform)<sup>244</sup> that modulates transcription or translation of the message<sup>248–250</sup>. The antibacterial ribocil was identified by a phenotypic screen for inhibitors of the riboflavin biosynthetic pathway in *E. coli*<sup>11</sup> (FIG. 5d and TABLE 1). Resistance mutations mapped to the FMN riboswitch immediately upstream of the *ribB* gene<sup>11,251</sup>, validating the RNA target and elucidating compound MOA.

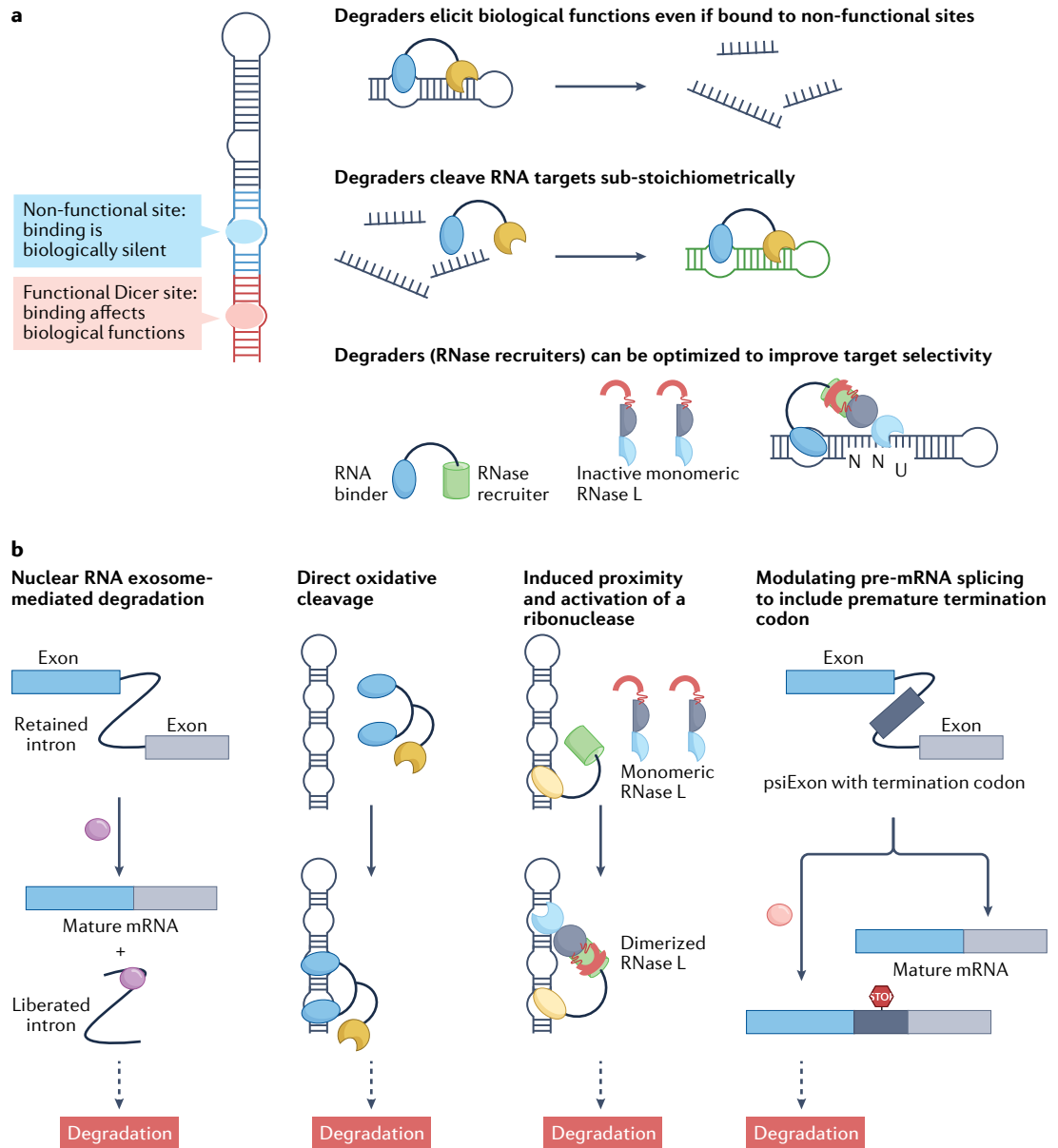


**Fig. 6 | Small-molecule RNA degraders and their mechanisms of action.** **a** | Degraders can elicit biological functions even if bound to non-functional sites within the RNA target as they cleave the transcript. Simply binding to non-functional sites is in principle biologically silent. Notably, degraders cleave RNA targets sub-stoichiometrically, as the same degrader molecule can cleave more than one RNA transcript by substrate turnover and can be optimized to improve target selectivity, including linker length, substrate preference and cellular localization of the target. **b** | Mechanisms of small-molecule-facilitated degradation. From left to right: small molecules can bind to intronic RNA repeat expansions that are harboured as retained introns. This causes excision of the intron, which is decayed by the RNA exosome<sup>280</sup>; RNA-binding compounds can be appended to natural products such as bleomycin that can cause oxidative cleavage of RNA targets selectively; ribonuclease-targeting chimeras induce the proximity of ribonucleases to unnaturally target an RNA for destruction by native quality control pathways; and small molecules can affect pre-mRNA splicing to create a mature mRNA with included exons that contain premature termination codons that trigger decay via nonsense-mediated decay. RNase, ribonuclease.

A crystal structure of the riboswitch–ribocil complex revealed that the compound competitively binds to the FMN-binding pocket, using a similar, but not identical, binding mode.

A structure-guided approach to target the FMN riboswitch was also fruitful, yielding the compound 5FDQD (TABLE 1). Inspection of the crystal structures of the FMN-bound<sup>252</sup> and apo-riboswitch<sup>253</sup> revealed conformational changes in the RNA that occur upon FMN recognition. An iterative structure-based design strategy was pursued in which, first, structures were analysed for regions that could potentially accommodate chemical changes to FMN; second, a set of structure-guided derivatives was synthesized; third, productive binding was tested using chemical probing and in vitro transcription assays; and fourth, crystal structures of new lead compounds that emerged were determined<sup>254,255</sup>. The compound that resulted from these efforts, 5FDQD, is an analogue of FMN that binds to its RNA target with activity equipotent to that of the natural effector<sup>254,255</sup>. The bactericidal activity of this compound is highly selective for *Clostridium difficile* while having little effect upon diverse other bacteria commonly found in the gut microbiota<sup>254</sup>. Importantly, in mice, 5FDQD prevented lethal antibiotic-induced *C. difficile* infection, validating the use of a structure-guided approach to yield potent RNA-targeting therapeutics.

**Risdiplam and branaplam, small molecules that target an RNA–protein manifold to direct alternative pre-mRNA splicing.** SMA is a genetic disease caused by the deletion or mutation of the survival motor neuron 1 (*SMN1*) gene, which encodes a catalytic component of a complex responsible for assembly of small nuclear ribonucleoproteins (snRNPs) and hence the spliceosome. Its loss of function in SMA ultimately leads to the degradation of spinal motor neurons, muscle weakness, muscle atrophy and respiratory complications<sup>66,256</sup>. Fortunately, humans encode an *SMN1* parologue, *SMN2*, with the two genes differing by only two nucleotides, one in exon 7 and the other in exon 8. The single-nucleotide polymorphism in exon 7 disrupts a splicing enhancer, resulting in exclusion of *SMN2* exon 7 and reduction of the half-life of the encoded protein. If *SMN2* exon 7 alternative splicing could be directed towards inclusion, then *SMN2* could substitute functionally for loss of *SMN1* and hence as a treatment for SMA (FIG. 5e).

A phenotypic screen to discover small molecules that direct splicing of *SMN2* such that exon 7 is included identified an orally bioavailable compound, SMN-C3. Subsequent studies showed that SMN-C3 directed endogenous alternative splicing of *SMN2* and provided therapeutic benefits in an SMA mouse model, with limited off-target effects. A medicinal chemistry campaign around SMN-C3 generated risdiplam (Evrysdi; FIG. 5e and TABLE 3), the first small-molecule FDA-approved drug to treat SMA<sup>14</sup>.

The lead optimization process that afforded risdiplam highlights a traditional medicinal chemistry approach (FIG. 4c). After chemical optimization of SMN-C3 to avoid mutagenicity and to confer favourable pharmacokinetic

profiles, the preclinical candidate RG7800 was selected for advancement<sup>66,257</sup>. As RG7800 caused retinal degeneration<sup>14</sup>, a medicinal chemistry campaign began around key elements of the chemical structure, particularly with the goal to lower basicity, enhance potency, improve influx into the central nervous system and reduce compound metabolism. A virtual study of a library containing a pyridopyrimidinone central core and a right-hand-side imidazopyridazine fragment was carried out<sup>14</sup>. Risdiplam emerged from these compounds after a battery of preclinical tests showed high potency for directing *SMN2* splicing in vitro and in vivo, reduced basicity, no phototoxicity risk and no formation of active metabolites<sup>14</sup>.

The challenge was to identify the target of risdiplam and hence its MOA, later determined after a series of studies on a derivative dubbed SMN-C5. NMR spectroscopy revealed that SMN-C5 stabilized an adenosine bulge at the exon 7–intron junction<sup>149,258,259</sup>, acting as a molecular glue for the ternary complex formed with U1 snRNP, revealed by Chem-CLIP<sup>260</sup>.

The small molecule branaplam was also identified from a similar phenotypic screen of *SMN2* exon 7 alternative splicing, using a mini-gene reporter of a breast cancer 1 (BRCA1) exon 18 mutant that induces exon skipping as a counter-screen<sup>15</sup>. A series of studies using a related molecule, NVS-SM2, pinpointed that the molecule interacted with 21 nucleotides of the *SMN2* 5' splice site, in particular a GA sequence found at the end of exon 7, suggesting involvement of U1 snRNP. NVS-SM2 acts as a molecular glue, as U1 snRNP only bound to *SMN2* exon 7 when the small molecule was present<sup>15</sup>. Branaplam was later discovered to reduce mutant huntingtin (mHTT) protein levels by facilitating pseudo-exon inclusion in the *HTT* mRNA<sup>261</sup>. It is currently in clinical trial for the treatment of both SMA and Huntington disease.

The discoveries of risdiplam and branaplam are perhaps the best examples of successful phenotypic drug discovery efforts, as their development did not rely on a specific target but instead on a desired activity.

**Rocaglamide, a molecular glue that inhibits translation of polypurine-containing transcripts.** Molecular glues that affect the translation of specific mRNAs have also been identified by phenotypic screening, particularly for oncogenic mRNAs that promote proliferation<sup>262,263</sup>. Notable amongst several interesting compounds is rocaglamide, a member of the flavaquine family, a class of bioactive natural products<sup>264</sup> (FIG. 5f and TABLE 2). Rocaglamide has potent anti-tumour activity, specifically inhibiting the translation of a subset of transcripts with polypurine sequences in their 5'UTRs. The compound stabilizes the interaction between eukaryotic initiation factor 4A (eIF4A), an ATP-dependent DEAD-box RNA helicase, and mRNAs that depend on eIF4A binding to unwind them for translation<sup>265</sup>. Recent studies have afforded rocaglamide analogues with improved potency and physicochemical properties<sup>266–268</sup>. Thus, translation can be affected not only by small-molecule binding to an mRNA, but also by pharmacological stabilization of transient interactions between transcripts

Table 4 | Tools and challenges in developing small-molecule therapeutics targeting RNA

Development step	Tools	Challenges
Identify druggable RNA targets	Identify regions in an RNA target that are stably folded by using evolution and prediction restrained by structure mapping experiments  Hypothesize a MOA for a binding compound  Convert a binder into a degrader if binding alone is not functional	Validating a predicted RNA structure in cells and identifying factors to prioritize targets that are more easily drugged
Identify small molecule binders	Complete sequence-based design and identify on- and off-targets and routes for optimization  Screen compound collections to find binders, considering screening on- and off-targets	Defining chemotypes in compounds that bind RNA selectively  Performing quantitative structure–activity relationships for RNA targets
Evaluate bioactivity of small molecules in cells	Study the effect of RNA target-associated phenotypes and validate by using gain- or loss-of-function  Use Chem-CLIP to define cellular on- and off-targets and evaluate the selectivity on the transcriptome and the proteome; correlate Chem-CLIP with -omics studies to define optimization plan	Correlating binding to function is not straightforward as not all binders will be biologically functional
Structure-based lead design and optimization	Solve structure of complex by NMR spectroscopy and X-ray crystallography, etc.  Study pharmacophore model to define features in binding compounds and expand chemical space for target by using chemical similarity searching of pharmacophore and structure-based drug design	Structure-based drug design and docking for RNA is different than for protein, i.e., electrostatic interactions are a significant driver  Force fields need development, as there are limited examples of driving potency and specificity using these approaches
Evaluate efficacy and PK in animal models	Study disease defect in model organisms, including transgenic models  In vitro and in vivo PK assays are well established	Physicochemical properties that potently and specifically affect RNA are unknown; need to be open minded and empirical with compounds, especially those outside rule of five space  Studies in model organisms can be challenging especially for noncoding RNAs owing to differences in the human sequence and structure  Varied modes of action can complicate PK and pharmacodynamic profiles
Preclinical and clinical studies	Study compound activity in patient tissues, available through many repositories  RNA-seq can be incorporated into clinical development pipeline to study efficacy, toxicity, potential off-targets	Should the pipeline of tests used for oligonucleotide-based medicines be altered? Can this process be streamlined by using RNA-seq and other tools?  Differences in sequence and structure in human versus mouse or other species should be considered in efficacy and toxicity studies

MOA, mode of action; PK, pharmacokinetic(s); RNA-seq, RNA sequencing.

and translation factors, providing specific functional outcomes. Other compounds have been shown to have similar activities, suggesting that medicinal optimization of these compounds could provide small-molecule therapeutics<sup>264</sup>.

### The future of small-molecule targeting of RNA

First viewed as simply an intermediate between DNA and protein, a renaissance in RNA structure and function beginning in the 1980s revealed the complex roles of RNA in homeostasis and disease<sup>183,269–273</sup>. Although considered a challenging target, modulation of RNA function by structure-binding small molecules is becoming increasingly well established as therapeutically practical. However, tremendous gaps in knowledge remain (TABLE 4 and BOX 3).

In the protein world, there are target classes that are considered both druggable and undruggable, generally classified by the formation of ordered structures. There is currently not enough knowledge in the RNA world to be able to classify RNA targets; however, most, if not all, bioactive small molecules target stable, functional structures. By identifying regions with unusually stable structures that are evolutionarily conserved, we can gain insight into potential functional structures and expand the druggable transcriptome. Key to the discovery of small molecules that bind these sites is to hypothesize function and hence potential compound MOA. Once the hypothesis is formulated, it must be verified by gain- and loss-of-function studies, particularly the effect on phenotype. Fortunately, if binding alone is insufficient to modulate RNA function, the binding small molecule can be

**Box 3 | Accelerating development of small molecules targeting RNA**

Key to advancing the RNA-targeting and chemical biology fields is an established pipeline for target validation and MOA studies, a longstanding process for proteins. Compounds with ill-defined mechanism are of less utility in chemical probe and lead medicine development than those that have an established MOA. A pathway for target validation and MOA studies has been previously presented<sup>65</sup>. The first step in this process is to confirm that the RNA target of interest is indeed driving phenotype, if not previously validated from *in vitro* or *in vivo* studies. For miRNAs, forced expression of the miRNA precursor in cells should induce or enhance the observed phenotype, while treatment with an antagonir should alleviate it. Validation for other RNA classes can be completed analogously by forced expression or knockout with ASOs. Small molecules that bind to the target can then be designed or discovered as described above.

Compounds that bind selectively to an RNA target *in vitro* can be carried forward to cellular studies to investigate whether they have the desired effect on the RNA and its downstream pathways, including phenotype. The effect of the small molecule on the abundance of the target RNA will depend on the target and the MOA of the compound. For example, small molecules that inhibit miRNA biogenesis by simply binding should boost levels of the precursor that it binds, leading to reduction of mature miRNA abundance. Small molecules that degrade the RNA target, whether directly or by recruiting nuclease, should reduce abundance. Further investigation is therefore required when an unexpected effect on RNA abundance is observed to define the compound's MOA and rule out other effects such as inhibition of transcription. Notably, small molecule binding can alert RNA surveillance and quality control pathways that could induce degradation, and thus an unexpected effect on abundance does not necessarily eliminate an RNA-centric MOA. Instead, cellular target engagement should be confirmed using the methods described above, as should be the case for all RNA-targeting endeavours.

To fully define the effect of an RNA-targeting small molecule on phenotype, gain-and loss-of-function studies should be completed. For the former, forced expression of the RNA target is expected to reduce compound efficacy, as less of the target can be occupied at the same dose. Loss-of-function studies is a multistep process that is MOA-dependent. The first step, regardless of RNA target or MOA, is to express the wild-type RNA and an RNA with point mutations that ablate the binding site of the small molecule in cells with low or no endogenous expression. Here, the small molecule should only alleviate molecular defects and phenotype in wild-type RNA-expressing cells. The second step, applied to all RNA targets, is to confirm that the small molecule has no effect on cells that do not (aberrantly) express the target, typically cells derived from healthy patients. The remaining steps in loss-of-function studies are tailored to compound MOA. For example, bioactive small molecules that modulate miRNA function derepress a downstream protein target that alleviates phenotype. The downstream target can be knocked out chemically or with a small interfering RNA. The small molecule is no longer able to boost abundance of the downstream target and hence alleviate phenotype.

converted into a degrader. As more data are collected around functional structures, we will be able to tease out factors that contribute to druggability.

Complementary to identifying high-priority RNA targets is defining physicochemical properties and chemotypes that confer affinity for RNA, which will inform design of RNA-focused small-molecule libraries (BOX 1). Such libraries can be used in two ways: first, sequence-based design by defining binding landscapes, which defines both on- and off-targets; and second, screening against defined targets, in which an appropriate counter-screen must be completed to improve the likelihood of selective binding. The resultant datasets refine hypotheses around physicochemical properties and chemotypes that are ideal for RNA targets and hence RNA-focused small-molecule libraries. Notably, these screening collections must maintain chemical diversity to be useful.

Advances in structure-based design and lead optimization for RNA-targeted small molecules are also

needed. Force fields that have been developed to enable structure-based design for proteins have not yet been fully customized for RNA, despite recent advances in computational biology. Molecular recognition of RNA by small molecules is driven differently than for protein, specifically the importance of aromatic ring stacking interactions that will require modification of electrostatic parameters. Accurate modelling of electrostatic parameters is key to understanding how small-molecule cores bind to and interact with an RNA target and to guide positioning of functionalities outside the core. Further, small-scale conformational dynamics are important for recognition of RNA targets. In its native state, RNA can have fast exchange between conformations, which are recognized by ligands differently. When the energetic difference between these states is low, there is likely only a modest effect on affinity. When the energy difference between conformations is large, however, the difference in affinity could be dramatic. Such knowledge is key for structure-based design.

Small-molecule binding is often not sufficient for bioactivity. Determining whether binding occurred to the cellular target but produced a biologically silent interaction is now possible with recently developed tools. Correlating target occupancy studies, using methods such as Chem-CLIP, with transcriptome- and proteome-wide studies is a powerful strategy that defines on- and off-targets and when binding elicits a biological response that is not desired. Such data are key to inform lead optimization. Intriguingly, fragment mapping and Chem-CLIP<sup>108,133,274</sup>, in combination with RNA structure prediction programs such as ScanFold, can provide insight into ligandable cellular RNA structures; biologically silent interactions inform cellular RNAs amenable to targeting by small-molecule-induced degradation.

Translating bioactive small molecules from cells to animals and then to the clinic is a significant hurdle for RNA-targeted small molecules. Of importance will be incorporation of transcriptome-wide analyses in patient tissues that assess efficacy and toxicity into clinical development pipelines, which should also be implemented for oligonucleotide-based modalities. Such studies also inform the range of selectivity that will be acceptable for RNA targets and may be quite different from that of proteins. For *in vivo* studies, significant differences in the sequence and structure of human and mouse RNAs, particularly noncoding RNAs, can change the activity or selectivity of a compound. As very few RNA-targeted compounds have advanced to animal studies and the clinic, more data will be needed to define pharmacokinetic and pharmacodynamic profiles ideal for preclinical and clinical candidates. As PROTACs and other protein-targeted medicines have changed the view of the rule of five<sup>275</sup>, we will need to be open to the fact that the physicochemical properties of small molecules that modulate RNA function may be outside the traditional drug-like space.

**Outlook**

As the functions of RNA in both health and disease have expanded and diversified, so has the field of RNA chemical biology, demonstrating that RNA is indeed

druggable by small molecules. Further, RNA-targeted small molecules can be designed and lead optimized, the latter using strategies developed for protein targets with important modifications and considerations. As both academia and industry push the frontiers of

this field forward, we believe that many more RNA-targeted medicines will reach the clinic in the years to come.

Published online: 08 August 2022

1. Jones, D., Metzger, H. J., Schatz, A. & Waksman, S. A. Control of Gram-negative bacteria in experimental animals by streptomycin. *Science* **100**, 103–105 (1944).
2. Waksman, S. A., Reilly, H. C. & Schatz, A. Strain specificity and production of antibiotic substances: V. Strain resistance of bacteria to antibiotic substances, especially to streptomycin. *Proc. Natl Acad. Sci. USA* **31**, 157–164 (1945).
3. Holley, R. W. et al. Structure of a ribonucleic acid. *Science* **147**, 1462 (1965).
4. Zaug, A. J. & Cech, T. R. The intervening sequence RNA of *Tetrahymena* is an enzyme. *Science* **231**, 470–475 (1986).
5. Stark, B. C., Kole, R., Bowman, E. J., Altman, S. & Altman, S. Ribonuclease P: an enzyme with an essential RNA component. *Proc. Natl Acad. Sci. USA* **75**, 3717–3721 (1978).
6. Encode Project Consortium. An integrated encyclopedia of DNA elements in the human genome. *Nature* **489**, 57–74 (2012).
7. Tsai, M. C. et al. Long noncoding RNA as modular scaffold of histone modification complexes. *Science* **329**, 689–693 (2010).
8. He, L. & Hannon, G. J. MicroRNAs: small RNAs with a big role in gene regulation. *Nat. Rev. Genet.* **5**, 522–531 (2004).
9. Bennett, C. F. Therapeutic antisense oligonucleotides are coming of age. *Annu. Rev. Med.* **70**, 307–321 (2019).
10. Luther, D. C., Lee, Y. W., Nagaraj, H., Scaletti, F. & Rotello, V. M. Delivery approaches for CRISPR/Cas9 therapeutics in vivo: advances and challenges. *Expert Opin. Drug Deliv.* **15**, 905–913 (2018).
11. Howe, J. A. et al. Selective small-molecule inhibition of an RNA structural element. *Nature* **526**, 672–677 (2015). **Describes the discovery of ribocil, a selective chemical modulator of bacterial riboflavin riboswitches.**
12. Dibrov, S. M. et al. Hepatitis C virus translation inhibitors targeting the internal ribosomal entry site. *J. Med. Chem.* **57**, 1694–1707 (2014).
13. Zhang, P. et al. Translation of the intrinsically disordered protein alpha-synuclein is inhibited by a small molecule targeting its structured mRNA. *Proc. Natl Acad. Sci. USA* **117**, 1457–1467 (2020). **Describes the design of a small molecule that inhibits the translation of the undruggable, intrinsically disordered protein α-synuclein by targeting its mRNA.**
14. Ratni, H. et al. Discovery of risdiplam, a selective survival of motor neuron-2 (SMN2) gene splicing modifier for the treatment of spinal muscular atrophy (SMA). *J. Med. Chem.* **61**, 6501–6517 (2018). **Discovery of the first FDA-approved small molecule (risdiplam) for the treatment of SMA by directing the alternative splicing of SMN2 to produce a functionally equivalent SMN1 protein.**
15. Palacino, J. et al. SMN2 splice modulators enhance U1-pre-mRNA association and rescue SMA mice. *Nat. Chem. Biol.* **12**, 304–304 (2016). **The discovery of the SMN2 splicing modulator branaplam for the treatment of SMA.**
16. Becquart, C. et al. Exploring heterocycle-spermine conjugates as modulators of oncogenic microRNAs biogenesis. *ACS Omega* **3**, 16500–16508 (2018). **Design of a heterocycle–spermine conjugate that inhibits the biogenesis of oncogenic miRNAs.**
17. Turner, D. H. & Mathews, D. H. NNDB: the nearest neighbor parameter database for predicting stability of nucleic acid secondary structure. *Nucleic Acids Res.* **38**, D280–D282 (2010).
18. Tinoco, I. Jr., Uhlenbeck, O. C. & Levine, M. D. Estimation of secondary structure in ribonucleic acids. *Nature* **230**, 362–367 (1971).
19. Freier, S. M. et al. Improved free-energy parameters for predictions of RNA duplex stability. *Proc. Natl Acad. Sci. USA* **83**, 9373–9377 (1986).
20. Zuker, M. mFold web server for nucleic acid folding and hybridization prediction. *Nucleic Acids Res.* **31**, 3406–3415 (2003).
21. Lorenz, R. et al. ViennaRNA Package 2.0. *Algorithms Mol. Biol.* **6**, 26 (2011).
22. Mathews, D. H. et al. Incorporating chemical modification constraints into a dynamic programming algorithm for prediction of RNA secondary structure. *Proc. Natl Acad. Sci. USA* **101**, 7287–7292 (2004).
23. Peattie, D. A. Direct chemical method for sequencing RNA. *Proc. Natl Acad. Sci. USA* **76**, 1760–1764 (1979).
24. Bevilacqua, P. C., Ritchey, L. E., Su, Z. & Assmann, S. M. Genome-wide analysis of RNA secondary structure. *Annu. Rev. Genet.* **50**, 235–266 (2016).
25. Sun, L. et al. RNA structure maps across mammalian cellular compartments. *Nat. Struct. Mol. Biol.* **26**, 322–330 (2019).
26. Marinus, T., Fessler, A. B., Ogle, C. A. & Incarnato, D. A novel SHAPE reagent enables the analysis of RNA structure in living cells with unprecedented accuracy. *Nucleic Acids Res.* **49**, e34 (2021).
27. Deigan, K. E., Li, T. W., Mathews, D. H. & Weeks, K. M. Accurate SHAPE-directed RNA structure determination. *Proc. Natl Acad. Sci. USA* **106**, 97–102 (2009).
28. Wells, S. E., Hughes, J. M., Igel, A. H. & Ares, M. Jr. Use of dimethyl sulfate to probe RNA structure in vivo. *Methods Enzymol.* **318**, 479–493 (2000).
29. Spitalte, R. C., Flynn, R. A., Torre, E. A., Kool, E. T. & Chang, H. Y. RNA structural analysis by evolving SHAPE chemistry. *Wiley Interdiscip. Rev. RNA* **5**, 867–881 (2014).
30. Eddy, S. R. Computational analysis of conserved RNA secondary structure in transcriptomes and genomes. *Annu. Rev. Biophys.* **43**, 433–456 (2014).
31. Eddy, S. R. & Durbin, R. RNA sequence analysis using covariance models. *Nucleic Acids Res.* **22**, 2079–2088 (1994).
32. Gutell, R. R., Lee, J. C. & Cannone, J. J. The accuracy of ribosomal RNA comparative structure models. *Curr. Opin. Struct. Biol.* **12**, 301–310 (2002).
33. Woese, C. R., Gutell, R., Gupta, R. & Noller, H. F. Detailed analysis of the higher-order structure of 16S-like ribosomal ribonucleic acids. *Microbiol. Rev.* **47**, 621–669 (1983).
34. Mathews, D. H. & Turner, D. H. Dynalign: an algorithm for finding the secondary structure common to two RNA sequences. *J. Mol. Biol.* **317**, 191–203 (2002).
35. Havgaard, J. H., Lyngso, R. B. & Gorodkin, J. The FOLDALIGN web server for pairwise structural RNA alignment and mutual motif search. *Nucleic Acids Res.* **33**, W650–W653 (2005).
36. Hofacker, I. L., Fekete, M. & Stadler, P. F. Secondary structure prediction for aligned RNA sequences. *J. Mol. Biol.* **319**, 1059–1066 (2002).
37. Watkins, A. M., Rangan, R. & Das, R. FARFAR2: improved de novo Rosetta prediction of complex global RNA folds. *Structure* **28**, 963–976 (2020).
38. Parisien, M. & Major, F. The MC-Fold and MC-Sym pipeline infers RNA structure from sequence data. *Nature* **452**, 51–55 (2008).
39. Sharma, S., Ding, F. & Dokholyan, N. V. iFoldRNA: three-dimensional RNA structure prediction and folding. *Bioinformatics* **24**, 1951–1952 (2008).
40. Capriotti, E., Norambuena, T., Martí-Renom, M. A. & Melo, F. All-atom knowledge-based potential for RNA structure prediction and assessment. *Bioinformatics* **27**, 1086–1093 (2011).
41. Townsend, J. L. et al. Geometric deep learning of RNA structure. *Science* **373**, 1047–1051 (2021).
42. Furtig, B., Richter, C., Wöhner, J. & Schwalbe, H. NMR spectroscopy of RNA. *ChemBioChem* **4**, 936–962 (2003).
43. Lietzke, S. E., Barnes, C. L. & Kundrot, C. E. Crystallization and structure determination of RNA. *Curr. Opin. Struct. Biol.* **5**, 645–649 (1995).
44. Spahn, C. M. & Penczek, P. A. Exploring conformational modes of macromolecular assemblies by multiparticle cryo-EM. *Curr. Opin. Struct. Biol.* **19**, 623–631 (2009).
45. Zhang, K. et al. Cryo-EM structure of a 40 kDa SAM-IV riboswitch RNA at 3.7 Å resolution. *Nat. Commun.* **10**, 5511 (2019).
46. Kappel, K. et al. Accelerated cryo-EM-guided determination of three-dimensional RNA-only structures. *Nat. Methods* **17**, 699–707 (2020).
47. Ding, Y., Chan, C. Y. & Lawrence, C. E. Sfold web server for statistical folding and rational design of nucleic acids. *Nucleic Acids Res.* **32**, W135–W141 (2004).
48. Do, C. B., Woods, D. A. & Batzoglou, S. CONTRAfold: RNA secondary structure prediction without physics-based models. *Bioinformatics* **22**, e90–e98 (2006).
49. Rivas, E., Clements, J. & Eddy, S. R. A statistical test for conserved RNA structure shows lack of evidence for structure in lncRNAs. *Nat. Methods* **14**, 45–48 (2017). **A statistical method that evaluates the functional relevance of a given RNA structure based on its phylogenetic conservation.**
50. Nawrocki, E. P. et al. Rfam 12.0: updates to the RNA families database. *Nucleic Acids Res.* **43**, D130–D137 (2015).
51. Fang, R., Moss, W. N., Rutenberg-Schoenberg, M. & Simon, M. D. Probing Xist RNA structure in cells using targeted structure-Seq. *PLoS Genet.* **11**, e1005668 (2015).
52. Somarowthu, S. et al. HOTAIR forms an intricate and modular secondary structure. *Mol. Cell* **58**, 353–361 (2015).
53. Novikova, I. V., Hennelly, S. P. & Sanbonmatsu, K. Y. Structural architecture of the human long non-coding RNA, steroid receptor RNA activator. *Nucleic Acids Res.* **40**, 5034–5051 (2012).
54. Rivas, E., Clements, J. & Eddy, S. R. Estimating the power of sequence covariation for detecting conserved RNA structure. *Bioinformatics* **36**, 3072–3076 (2020).
55. Rouskin, S., Zubradt, M., Washietl, S., Kellis, M. & Weissman, J. S. Genome-wide probing of RNA structure reveals active unfolding of mRNA structures in vivo. *Nature* **505**, 701–705 (2014).
56. Ding, Y. et al. In vivo genome-wide profiling of RNA secondary structure reveals novel regulatory features. *Nature* **505**, 696–700 (2014).
57. Wan, Y. et al. Landscape and variation of RNA secondary structure across the human transcriptome. *Nature* **505**, 706–709 (2014).
58. Sobczak, K. & Krzyzosiak, W. J. CAG repeats containing CAA interruptions form branched hairpin structures in spinocerebellar atrophy type 2 transcripts. *J. Biol. Chem.* **280**, 3898–3910 (2005).
59. Busan, S. & Weeks, K. M. Role of context in RNA structure: flanking sequences reconfigure CAG motif folding in huntingtin exon 1 transcripts. *Biochemistry* **52**, 8219–8225 (2013).
60. Kole, R., Krainer, A. R. & Altman, S. RNA therapeutics: beyond RNA interference and antisense oligonucleotides. *Nat. Rev. Drug Discov.* **11**, 125–140 (2012).
61. Sudarsan, N., Barrick, J. E. & Breaker, R. R. Metabolite-binding RNA domains are present in the genes of eukaryotes. *RNA* **9**, 644–647 (2003).
62. Andrews, R. J., Roche, J. & Moss, W. N. ScanFold: an approach for genome-wide discovery of local RNA structural elements—applications to Zika virus and HIV. *PeerJ* **6**, e6136 (2018).
63. Moss, W. N., Priore, S. F. & Turner, D. H. Identification of potential conserved RNA secondary structure throughout influenza A coding regions. *RNA* **17**, 991–1011 (2011).
64. O’Leary, C. et al. RNA structural analysis of the MYC mRNA reveals conserved motifs that affect gene expression. *PLoS ONE* **14**, e0213758 (2019).
65. Disney, M. D. Targeting RNA with small molecules to capture opportunities at the intersection of chemistry, biology, and medicine. *J. Am. Chem. Soc.* **141**, 6776–6790 (2019). **Describes the sequence-based design of RNA structure-specific small molecules, including the 2DCS selection platform as well as target validation techniques.**
66. Narayshkin, N. A. et al. Motor neuron disease. SMN2 splicing modifiers improve motor function and

- longevity in mice with spinal muscular atrophy. *Science* **345**, 688–693 (2014).
67. Parsons, J. et al. Conformational inhibition of the hepatitis C virus internal ribosome entry site RNA. *Nat. Chem. Biol.* **5**, 823–825 (2009).
  68. Carnevali, M., Parsons, J., Wyles, D. L. & Hermann, T. A modular approach to synthetic RNA binders of the hepatitis C virus internal ribosome entry site. *ChemBioChem* **11**, 1364–1367 (2010).
  69. Chen, C. Z. et al. Two high-throughput screening assays for aberrant RNA–protein interactions in myotonic dystrophy type 1. *Anal. Bioanal. Chem.* **402**, 1889–1898 (2012).
  70. Chen, J. L. et al. Design, optimization, and study of small molecules that target tau pre-mRNA and affect splicing. *J. Am. Chem. Soc.* **142**, 8706–8727 (2020).
  71. Corbett, P. T. et al. Dynamic combinatorial chemistry. *Chem. Rev.* **106**, 3652–3711 (2006).
  72. Motoyaji, T. Revolution of small molecule drug discovery by affinity selection–mass spectrometry technology. *Chem. Pharm. Bull.* **68**, 191–193 (2020).
  73. Kiernan, U. A., Nedelkov, D., Niederkofler, E. E., Tubbs, K. A. & Nelson, R. W. High-throughput affinity mass spectrometry. *Methods Mol. Biol.* **328**, 141–150 (2006).
  74. Annis, D. A. et al. An affinity selection–mass spectrometry method for the identification of small molecule ligands from self-encoded combinatorial libraries. *Int. J. Mass. Spectrom.* **238**, 77–83 (2004).
  75. Rizvi, N. F. et al. Discovery of selective RNA-binding small molecules by affinity-selection mass spectrometry. *ACS Chem. Biol.* **13**, 820–831 (2018).
  76. Rizvi, N. F. & Nickbarg, E. B. RNA-ALIS: methodology for screening soluble RNAs as small molecule targets using ALIS affinity-selection mass spectrometry. *Methods* **167**, 28–38 (2019).
  77. Stover, J. S., Shi, J., Jin, W., Vogt, P. K. & Boger, D. L. Discovery of inhibitors of aberrant gene transcription from libraries of DNA binding molecules: inhibition of LEF-1-mediated gene transcription and oncogenic transformation. *J. Am. Chem. Soc.* **131**, 3342–3348 (2009).
  78. Tran, T. & Disney, M. D. Identifying the preferred RNA motifs and chemotypes that interact by probing millions of combinations. *Nat. Commun.* **3**, 1125 (2012).
  79. Asare-Okai, P. N. & Chow, C. S. A modified fluorescent intercalator displacement assay for RNA ligand discovery. *Anal. Biochem.* **408**, 269–276 (2011). **Demonstrates the successful application of ALIS to RNA targets.**
  80. Wang, Z. F. et al. The hairpin form of r(G,C)<sub>n</sub><sup>exp</sup> in c9ALS/FTD is repeat-associated non-ATG translated and a target for bioactive small molecules. *Cell Chem. Biol.* **26**, 179–190 (2019).
  81. Zhang, J., Umemoto, S. & Nakatani, K. Fluorescent indicator displacement assay for ligand-RNA interactions. *J. Am. Chem. Soc.* **132**, 3660–3661 (2010).
  82. Wicks, S. L. & Hargrove, A. E. Fluorescent indicator displacement assays to identify and characterize small molecule interactions with RNA. *Methods* **167**, 3–14 (2019).
  83. Jones, A. C. & Neely, R. K. 2-Aminopurine as a fluorescent probe of DNA conformation and the DNA-enzyme interface. *Q. Rev. Biophys.* **48**, 244–279 (2015).
  84. Jean, J. M. & Hall, K. B. 2-Aminopurine fluorescence quenching and lifetimes: role of base stacking. *Proc. Natl. Acad. Sci. USA* **98**, 37–41 (2001).
  85. Soulière, M. F., Haller, A., Rieder, R. & Micura, R. A powerful approach for the selection of 2-aminopurine substitution sites to investigate RNA folding. *J. Am. Chem. Soc.* **133**, 16161–16167 (2011).
  86. Soulière, M. F. & Micura, R. Use of SHAPE to select 2AP substitution sites for RNA-ligand interactions and dynamics studies. *Methods Mol. Biol.* **1103**, 227–239 (2014).
  87. Froeyen, M. & Heredewijn, P. RNA as a target for drug design, the example of Tat-TAR interaction. *Curr. Top. Med. Chem.* **2**, 1123–1145 (2002).
  88. Pascale, L. et al. Deciphering structure-activity relationships in a series of Tat/TAR inhibitors. *J. Biomol. Struct. Dyn.* **34**, 2327–2338 (2016).
  89. Yang, M. Discoveries of Tat-TAR interaction inhibitors for HIV-1. *Curr. Drug Targets Infect. Disord.* **5**, 433–444 (2005).
  90. Kumar, A. et al. Chemical correction of pre-mRNA splicing defects associated with sequestration of muscleblind-like 1 protein by expanded r(CAG)-containing transcripts. *ACS Chem. Biol.* **7**, 496–505 (2012).
  91. MacBeath, G., Koehler, A. N. & Schreiber, S. L. Printing small molecules as microarrays and detecting protein–ligand interactions en masse. *J. Am. Chem. Soc.* **121**, 7967–7968 (1999).
  92. Fazio, F., Bryan, M. C., Blixt, O., Paulson, J. C. & Wong, C. H. Synthesis of sugar arrays in microtiter plate. *J. Am. Chem. Soc.* **124**, 14397–14402 (2002).
  93. Peng, B., Thorsell, A. G., Karlberg, T., Schuler, H. & Yao, S. Q. Small molecule microarray based discovery of PARP14 inhibitors. *Angew. Chem. Int. Ed. Engl.* **56**, 248–253 (2017).
  94. Wang, Z. et al. Microarray based screening of peptide nano probes for HER2 positive tumor. *Anal. Chem.* **87**, 8367–8372 (2015).
  95. Disney, M. D. & Seeberger, P. H. Aminoglycoside microarrays to explore interactions of antibiotics with RNAs and proteins. *Chemistry* **10**, 3308–3314 (2004).
  96. Disney, M. D. & Barrett, O. J. An aminoglycoside microarray platform for directly monitoring and studying antibiotic resistance. *Biochemistry* **46**, 11223–11230 (2007).
  97. Abulwerdi, F. A. et al. Selective small-molecule targeting of a triple helix encoded by the long noncoding RNA, MALAT1. *ACS Chem. Biol.* **14**, 223–235 (2019).
  98. Connally, C. M., Abulwerdi, F. A. & Schneekloth, J. S. Jr. Discovery of RNA binding small molecules using small molecule microarrays. *Methods Mol. Biol.* **1518**, 157–175 (2017). **A detailed description of a small molecule microarray method for the identification of small-molecule RNA binders.**
  99. Connally, C. M., Boer, R. E., Moon, M. H., Gareiss, P. & Schneekloth, J. S. Jr. Discovery of inhibitors of microRNA-21 processing using small molecule microarrays. *ACS Chem. Biol.* **12**, 435–443 (2017).
  100. Connally, C. M. et al. Synthetic ligands for PreQ(1) riboswitches provide structural and mechanistic insights into targeting RNA tertiary structure. *Nat. Commun.* **10**, 1501 (2019). **An example of how structural studies can enhance the understanding of ligand binding and function, in the context of PreQ1 riboswitch.**
  101. Sztuba-Solinska, J. et al. Identification of biologically active, HIV TAR RNA-binding small molecules using small molecule microarrays. *J. Am. Chem. Soc.* **136**, 8402–8410 (2014). **A successful application of small-molecule microarray for the discovery of a HIV-1 TAR RNA binder.**
  102. Tran, B. et al. Parallel discovery strategies provide a basis for riboswitch ligand design. *Cell Chem. Biol.* **27**, 1241–1249.e1244 (2020).
  103. Labuda, L. P., Pushechnikov, A. & Disney, M. D. Small molecule microarrays of RNA-focused peptoids help identify inhibitors of a pathogenic group I intron. *ACS Chem. Biol.* **4**, 299–307 (2009).
  104. Velagapudi, S. P. et al. Approved anti-cancer drugs target oncogenic non-coding RNAs. *Cell Chem. Biol.* **25**, 1086–1094.e1087 (2018).
  105. Sreramulu, S. et al. Exploring the druggability of conserved RNA regulatory elements in the SARS-CoV-2 genome. *Angew. Chem. Int. Ed. Engl.* **60**, 19191–19200 (2021).
  106. Parker, C. G. et al. Ligand and target discovery by fragment-based screening in human cells. *Cell* **168**, 527–541.e529 (2017).
  107. Wang, Y. et al. Expedited mapping of the ligandable proteome using fully functionalized enantiomeric probe pairs. *Nat. Chem.* **11**, 1113–1123 (2019).
  108. Suresh, B. M. et al. A general fragment-based approach to identify and optimize bioactive ligands targeting RNA. *Proc. Natl. Acad. Sci. USA* **117**, 33197–33203 (2020). **The first application of fully functionalized fragments to the discovery of RNA ligands.**
  109. Benhamou, R. I. et al. DNA-encoded library-versus-RNA-encoded library selection enables design of an oncogenic non-coding RNA inhibitor. *Proc. Natl. Acad. Sci. USA* **119**, e2114971119 (2022).
  110. Litovchick, A. et al. Novel nucleic acid binding small molecules discovered using DNA-encoded chemistry. *Molecules* **24**, 2026 (2019).
  111. Disney, M. D., Velagapudi, S. P., Li, Y., Costales, M. G. & Childs-Dysney, J. L. Identifying and validating small molecules interacting with RNA (SMIRNAs). *Methods Enzymol.* **623**, 45–66 (2019).
  112. Disney, M. D. et al. Two-dimensional combinatorial screening identifies specific aminoglycoside-RNA internal loop partners. *J. Am. Chem. Soc.* **130**, 11185–11194 (2008).
  113. Costales, M. G., Childs-Dysney, J. L., Haniff, H. S. & Disney, M. D. How we think about targeting RNA with small molecules. *J. Med. Chem.* **63**, 8880–8900 (2020).
  114. Velagapudi, S. P. et al. Defining RNA-small molecule affinity landscapes enables design of a small molecule inhibitor of an oncogenic noncoding RNA. *ACS Cent. Sci.* **3**, 205–216 (2017).
  115. Thomas, J. R. & Hergenrother, P. J. Targeting RNA with small molecules. *Chem. Rev.* **108**, 1171–1224 (2008).
  116. Kuntz, I. D. Structure-based strategies for drug design and discovery. *Science* **257**, 1078–1082 (1992).
  117. Sledz, P. & Caflisch, A. Protein structure-based drug design: from docking to molecular dynamics. *Curr. Opin. Struct. Biol.* **48**, 93–102 (2018).
  118. Yadav, M., Dhagat, S. & Eswari, J. S. Structure based drug design and molecular docking studies of anticancer molecules paclitaxel, etoposide and topotecan using novel ligands. *Curr. Drug Discov. Technol.* **17**, 183–190 (2020).
  119. Batool, M., Ahmad, B. & Choi, S. A structure-based drug discovery paradigm. *Int. J. Mol. Sci.* **20**, 2783 (2019).
  120. Ganser, L. R. et al. Probing RNA conformational equilibria within the functional cellular context. *Cell Rep.* **30**, 2472–2480 (2020). **An NMR-based method that assesses the energetic properties of transient RNA conformations in vitro.**
  121. Ganser, L. R. et al. High-performance virtual screening by targeting a high-resolution RNA dynamic ensemble. *Nat. Struct. Mol. Biol.* **25**, 425–434 (2018).
  122. Shi, H. et al. Rapid and accurate determination of atomistic RNA dynamic ensemble models using NMR and structure prediction. *Nat. Commun.* **11**, 5531 (2020).
  123. Liu, B., Shi, H. & Al-Hashimi, H. M. Developments in solution-state NMR yield broader and deeper views of the dynamic ensembles of nucleic acids. *Curr. Opin. Struct. Biol.* **70**, 16–25 (2021).
  124. Zhang, Q., Sun, X., Watt, E. D. & Al-Hashimi, H. M. Resolving the motional modes that code for RNA adaptation. *Science* **311**, 653–656 (2006).
  125. Frank, A. T., Stelzer, A. C., Al-Hashimi, H. M. & Andricioaei, I. Constructing RNA dynamical ensembles by combining MD and motionally decoupled NMR RDCs: new insights into RNA dynamics and adaptive ligand recognition. *Nucleic Acids Res.* **37**, 3670–3679 (2009).
  126. Stelzer, A. C. et al. Discovery of selective bioactive small molecules by targeting an RNA dynamic ensemble. *Nat. Chem. Biol.* **7**, 553–559 (2011). **An example of using structural docking and virtual screening for the discovery of an HIV TAR RNA inhibitor.**
  127. Bush, J. A. et al. Systematically studying the effect of small molecules interacting with RNA in cellular and preclinical models. *ACS Chem. Biol.* **16**, 1111–1127 (2021).
  128. Winkler, W. C., Cohen-Chalamish, S. & Breaker, R. R. An mRNA structure that controls gene expression by binding FMN. *Proc. Natl. Acad. Sci. USA* **99**, 15908–15913 (2002).
  129. Sudarsan, N., Cohen-Chalamish, S., Nakamura, S., Emilsson, G. M. & Breaker, R. R. Thiamine pyrophosphate riboswitches are targets for the antimicrobial compound pyrithiamine. *Chem. Biol.* **12**, 1325–1335 (2005).
  130. Lin, A. et al. Off-target toxicity is a common mechanism of action of cancer drugs undergoing clinical trials. *Sci. Transl. Med.* **11**, eaaw8412 (2019).
  131. Osborn, M. F., White, J. D., Haley, M. M. & DeRose, V. J. Platinum-RNA modifications following drug treatment in *S. cerevisiae* identified by click chemistry and enzymatic mapping. *ACS Chem. Biol.* **9**, 2404–2411 (2014).
  132. Mortison, J. D. et al. Tetracyclines modify translation by targeting key human rRNA substructures. *Cell Chem. Biol.* **25**, 1506–1518 (2018).
  133. Balaratnam, S. et al. A chemical probe based on the PreQ1 metabolite enables transcriptome-wide mapping of binding sites. *Nat. Commun.* **12**, 5856 (2021).
  134. Guan, L. & Disney, M. D. Covalent small-molecule–RNA complex formation enables cellular profiling of small-molecule–RNA interactions. *Angew. Chem. Int. Ed. Engl.* **52**, 10010–10013 (2013).
  135. Zarrinkar, P. P., Wang, J. & Williamson, J. R. Slow folding kinetics of RNase P RNA. *RNA* **2**, 564–573 (1996).
  136. Zarrinkar, P. P. & Williamson, J. R. Kinetic intermediates in RNA folding. *Science* **265**, 918–924 (1994).

137. Boger, D. L. & Cai, H. Bleomycin: synthetic and mechanistic studies. *Angew. Chem. Int. Ed. Engl.* **38**, 448–476 (1999).
138. Ishida, R. & Takahashi, T. Increased DNA chain breakage by combined action of bleomycin and superoxide radical. *Biochem. Biophys. Res. Commun.* **66**, 1432–1438 (1975).
139. Burger, R. M. Cleavage of nucleic acids by bleomycin. *Chem. Rev.* **98**, 1153–1170 (1998).
140. Magliozzo, R. S., Peisach, J. & Ciriolo, M. R. Transfer-RNA is cleaved by activated bleomycin. *Mol. Pharmacol.* **35**, 428–432 (1989).
141. Carter, B. J. et al. Site-specific cleavage of RNA by Fe(II)-bleomycin. *Proc. Natl Acad. Sci. USA* **87**, 9373–9377 (1990).
142. Abraham, A. T., Lin, J. J., Newton, D. L., Rybak, S. & Hecht, S. M. RNA cleavage and inhibition of protein synthesis by bleomycin. *Chem. Biol.* **10**, 45–52 (2003).
143. Costales, M. G. et al. Small-molecule targeted recruitment of a nuclelease to cleave an oncogenic RNA in a mouse model of metastatic cancer. *Proc. Natl Acad. Sci. USA* **117**, 2406–2411 (2020).
144. Costales, M. G., Matsumoto, Y., Velagapudi, S. P. & Disney, M. D. Small molecule targeted recruitment of a nuclease to RNA. *J. Am. Chem. Soc.* **140**, 6741–6744 (2018).
145. Bisbal, C., Martinand, C., Silhol, M., Lebleu, B. & Salehzada, T. Cloning and characterization of a RNase L inhibitor: A new component of the interferon-regulated 2'-5'A pathway. *J. Biol. Chem.* **270**, 13308–13317 (1995).
146. Li, X. L. et al. RNase-L-dependent destabilization of interferon-induced mRNAs: A role for the 2'-5'A system in attenuation of the interferon response. *J. Biol. Chem.* **275**, 8880–8888 (2000).
147. Zhou, A., Molinaro, R. J., Malathi, K. & Silverman, R. H. Mapping of the human RNASEL promoter and expression in cancer and normal cells. *J. Interferon Cytokine Res.* **25**, 595–603 (2005).
148. Silverman, R. H. Viral encounters with 2',5'-oligoadenylate synthetase and RNase L during the interferon antiviral response. *J. Virol.* **81**, 12720–12729 (2007).
149. Meyer, S. M. et al. Small molecule recognition of disease-relevant RNA structures. *Chem. Soc. Rev.* **49**, 7167–7199 (2020).
150. Zhang, P. et al. Reprogramming of protein-targeted small-molecule medicines to RNA by ribonuclease recruitment. *J. Am. Chem. Soc.* **143**, 13044–13055 (2021).  
**Shows that known drugs can be reprogrammed to selectively target RNA by its conversion into a ribonuclease targeting chimera (RIBOTAC) degrader.**
151. Lorenz, M. O. Methods of measuring the concentration of wealth. *Publ. Am. Stat. Assoc.* **9**, 209–219 (1905).
152. Ursu, A. et al. Gini coefficients as a single value metric to define chemical probe selectivity. *ACS Chem. Biol.* **15**, 2031–2040 (2020).
153. Graczyk, P. P. Gini coefficient: a new way to express selectivity of kinase inhibitors against a family of kinases. *J. Med. Chem.* **50**, 5773–5779 (2007).
154. Fedorova, O. et al. Small molecules that target group II introns are potent antifungal agents. *Nat. Chem. Biol.* **14**, 1073–1078 (2018).  
**Explores the use of small molecules through high-throughput screening, SAR and lead optimization to target a fungal self-splicing group II intron.**
155. Anastasopoulou, P. et al. Synthesis of triazole-functionalized 2-DOS analogues and their evaluation as A-site binders. *Bioorg. Med. Chem. Lett.* **24**, 1122–1126 (2014).
156. Iwatani-Yoshihara, M. et al. Discovery of allosteric inhibitors targeting the spliceosomal RNA helicase Brr2. *J. Med. Chem.* **60**, 5759–5771 (2017).
157. Abuwerdi, F. A. et al. Development of small molecules with a noncanonical binding mode to HIV-1 trans activation response (TAR) RNA. *J. Med. Chem.* **59**, 11148–11160 (2016).
158. Seth, P. P. et al. SAR by MS: discovery of a new class of RNA-binding small molecules for the hepatitis C virus: internal ribosome entry site IIA subdomain. *J. Med. Chem.* **48**, 7099–7102 (2005).
159. Vo, D. D. et al. Oncogenic microRNAs biogenesis as a drug target: structure–activity relationship studies on new aminoglycoside conjugates. *Chemistry* **22**, 5350–5362 (2016).
160. Patwardhan, N. N. et al. Amiloride as a new RNA-binding scaffold with activity against HIV-1 TAR. *MedChemComm* **8**, 1022–1036 (2017).
161. Mammen, M., Choi, S.-K. & Whitesides, G. M. Polyvalent interactions in biological systems: implications for design and use of multivalent ligands and inhibitors. *Angew. Chem. Int. Ed.* **37**, 2754–2794 (1998).
162. Gestwicki, J. E., Cairo, C. W., Strong, L. E., Oetjen, K. A. & Kiessling, L. L. Influencing receptor-ligand binding mechanisms with multivalent ligand architecture. *J. Am. Chem. Soc.* **124**, 14922–14933 (2002).
163. Jahromi, A. H. et al. Developing bivalent ligands to target CUG triplet repeats, the causative agent of myotonic dystrophy type 1. *J. Med. Chem.* **56**, 9471–9481 (2013).
164. Pushechnikov, A. V. et al. Rational design of ligands targeting triplet repeating transcripts that cause RNA dominant disease: application to myotonic muscular dystrophy type 1 and spinocerebellar atrophy type 3. *J. Am. Chem. Soc.* **131**, 9767–9779 (2009).
165. Childs-Daisy, J. L., Hoskins, J., Rzucek, S. G., Thornton, C. A. & Disney, M. D. Rationally designed small molecules targeting the RNA that causes myotonic dystrophy type 1 are potently bioactive. *ACS Chem. Biol.* **7**, 856–862 (2012).
166. Thadke, S. A. et al. Design of bivalent nucleic acid ligands for recognition of RNA-repeated expansion associated with Huntington's disease. *Biochemistry* **57**, 2094–2108 (2018).
167. Velagapudi, S. P. et al. Design of a small molecule against an oncogenic noncoding RNA. *Proc. Natl Acad. Sci. USA* **113**, 5898–5903 (2016).
168. Le Grice, S. F. Targeting the HIV RNA genome: high-hanging fruit only needs a longer ladder. *Curr. Top. Microbiol. Immunol.* **389**, 147–169 (2015).
169. Zapp, M. L., Stern, S. & Green, M. R. Small molecules that selectively block RNA binding of HIV-1 rev protein inhibit Rev function and viral production. *Cell* **74**, 969–978 (1993).
170. Mei, H.-Y. et al. Inhibition of an HIV-1 Tat-derived peptide binding to TAR RNA by aminoglycoside antibiotics. *Bioorg. Med. Chem. Lett.* **5**, 2755–2760 (1995).
171. Wang, S., Huber, P. W., Cui, M., Czarnik, A. W. & Mei, H. Y. Binding of neomycin to the TAR element of HIV-1 RNA induces dissociation of Tat protein by an allosteric mechanism. *Biochemistry* **37**, 5549–5557 (1998).
172. Ratmeyer, L. et al. Inhibition of HIV-1 Rev–RRE interaction by diphenylfuran derivatives. *Biochemistry* **35**, 13689–13696 (1996).
173. Park, W. K. C., Auer, M., Jaksche, H. & Wong, C.-H. Rapid combinatorial synthesis of aminoglycoside antibiotic mimetics: use of a polyethylene glycol-linked amine and a neamine-derived aldehyde in multiple component condensation as a strategy for the discovery of new inhibitors of the HIV RNA Rev responsive element. *J. Am. Chem. Soc.* **118**, 10150–10155 (1996).
174. Mei, H. Y. et al. Inhibitors of protein–RNA complexation that target the RNA: specific recognition of human immunodeficiency virus type 1 TAR RNA by small organic molecules. *Biochemistry* **37**, 14204–14212 (1998).
175. Hellen, C. U. & Pestova, T. V. Translation of hepatitis C virus RNA. *J. Viral Hepat.* **6**, 79–87 (1999).
176. Ji, H., Fraser, C. S., Yu, Y., Leary, J. & Doudna, J. A. Coordinated assembly of human translation initiation complexes by the hepatitis C virus internal ribosome entry site RNA. *Proc. Natl Acad. Sci. USA* **101**, 16990–16995 (2004).
177. Otto, G. A. & Puglisi, J. D. The pathway of HCV IRES-mediated translation initiation. *Cell* **119**, 369–380 (2004).
178. Wang, W. et al. Hepatitis C viral IRES inhibition by phenazine and phenazine-like molecules. *Bioorg. Med. Chem. Lett.* **10**, 1151–1154 (2000).
179. Jefferson, E. A. et al. Biaryl guanidine inhibitors of in vitro HCV-IRES activity. *Bioorg. Med. Chem. Lett.* **14**, 5139–5143 (2004).
180. Dibrov, S. M. et al. Structure of a hepatitis C virus RNA domain in complex with a translation inhibitor reveals a binding mode reminiscent of riboswitches. *Proc. Natl Acad. Sci. USA* **109**, 5223–5228 (2012).
181. Zafferani, M. et al. Amilorides inhibit SARS-CoV-2 replication *in vitro* by targeting RNA structures. *Sci. Adv.* **7**, eab16096 (2021).  
**Identification of small molecules that inhibit SARS-CoV-2 viral replication by interacting with the 5'UTR of the viral mRNA.**
182. Michel, F. & Dujon, B. Conservation of RNA secondary structures in two intron families including mitochondrial-, chloroplast- and nuclear-encoded members. *EMBO J.* **2**, 33–38 (1983).
183. Fire, A. et al. Potent and specific genetic interference by double-stranded RNA in *Caenorhabditis elegans*. *Nature* **391**, 806–811 (1998).
184. Lee, R. C. & Ambros, V. An extensive class of small RNAs in *Caenorhabditis elegans*. *Science* **294**, 862–864 (2001).
185. Bushati, N. & Cohen, S. microRNA functions. *Annu. Rev. Cell Dev. Biol.* **23**, 175–205 (2007).
186. Warner, K. D., Hajdin, C. E. & Weeks, K. M. Principles for targeting RNA with drug-like small molecules. *Nat. Rev. Drug Discov.* **17**, 547–558 (2018).
187. Di Giorgio, A. & Duca, M. Synthetic small-molecule RNA ligands: future prospects as therapeutic agents. *MedChemComm* **10**, 1242–1255 (2019).
188. Disney, M. D. & Angelbello, A. J. Rational design of small molecules targeting oncogenic noncoding RNAs from sequence. *Acc. Chem. Res.* **49**, 2698–2704 (2016).
189. Pomplun, S., Gates, Z. P., Zhang, G., Quartararo, A. J. & Pentelute, B. L. Discovery of nucleic acid binding molecules from combinatorial biohybrid nucleobase peptide libraries. *J. Am. Chem. Soc.* **142**, 19642–19651 (2020).
190. Garner, A. L. et al. Tetracyclines as inhibitors of pre-microRNA maturation: a disconnection between RNA binding and inhibition. *ACS Med. Chem. Lett.* **10**, 816–821 (2019).
191. Di Giorgio, A., Tran, T. P. & Duca, M. Small-molecule approaches toward the targeting of oncogenic miRNAs: roadmap for the discovery of RNA modulators. *Future Med. Chem.* **8**, 803–816 (2016).
192. Staedel, C. et al. Modulation of oncogenic miRNA biogenesis using functionalized polyamines. *Sci. Rep.* **8**, 1667 (2018).
193. Maucort, C. et al. Design and implementation of synthetic RNA binders for the inhibition of miR-21 biogenesis. *ACS Med. Chem. Lett.* **12**, 899–906 (2021).
194. Costales, M. G. et al. A designed small molecule inhibitor of a non-coding RNA sensitizes HER2 negative cancers to herceptin. *J. Am. Chem. Soc.* **141**, 2960–2974 (2019).
195. Cox, A. D., Fesik, S. W., Kimmelman, A. C., Luo, J. & Der, C. J. Drugging the undruggable RAS: mission possible? *Nat. Rev. Drug Discov.* **13**, 828–851 (2014).
196. Dang, C. V., Reddy, E. P., Shokat, K. M. & Soucek, L. Drugging the ‘undruggable’ cancer targets. *Nat. Rev. Cancer* **17**, 502–508 (2017).
197. Zhou, Z. D. & Tan, E. K. Iron regulatory protein (IRP)-iron responsive element (IRE) signaling pathway in human neurodegenerative diseases. *Mol. Neurodegener.* **12**, 75 (2017).
198. Pantopoulos, K. Iron metabolism and the IRE/IRP regulatory system: an update. *Ann. N. Y. Acad. Sci.* **1012**, 1–13 (2004).
199. Volz, K. Conservation in the iron responsive element family. *Genes* **12**, 1365 (2021).
200. Muckenthaler, M. U., Galy, B. & Hentze, M. W. Systemic iron homeostasis and the iron-responsive element/iron-regulatory protein (IRE/IRP) regulatory network. *Annu. Rev. Nutr.* **28**, 197–213 (2008).
201. Maio, N. et al. Mechanisms of cellular iron sensing, regulation of erythropoiesis and mitochondrial iron utilization. *Semin. Hematol.* **58**, 161–174 (2021).
202. Shaw, K. T. et al. Phenserine regulates translation of beta-amyloid precursor protein mRNA by a putative interleukin-1 responsive element, a target for drug development. *Proc. Natl Acad. Sci. USA* **98**, 7605–7610 (2001).
203. Rogers, J. T. & Cahill, C. M. Iron-responsive-like elements and neurodegenerative ferroptosis. *Learn. Mem.* **27**, 395–413 (2020).
204. Lumsden, A. L. et al. Dysregulation of neuronal iron homeostasis as an alternative unifying effect of mutations causing familial Alzheimer’s disease. *Front. Neurosci.* **12**, 533 (2018).
205. Rogers, J. T. et al. An iron-responsive element type II in the 5'-untranslated region of the Alzheimer’s amyloid precursor protein transcript. *J. Biol. Chem.* **277**, 45518–45528 (2002).
206. Zhang, P. et al. Ferroptosis was more initial in cell death caused by iron overload and its underlying mechanism in Parkinson’s disease. *Free Radic. Biol. Med.* **152**, 227–234 (2020).
207. Olivares, D., Huang, X., Branden, L., Greig, N. H. & Rogers, J. T. Physiological and pathological role of alpha-synuclein in Parkinson’s disease through iron mediated oxidative stress; the role of a putative iron-responsive element. *Int. J. Mol. Sci.* **10**, 1226–1260 (2009).

208. Bandyopadhyay, S. et al. Novel 5' untranslated region directed blockers of iron-regulatory protein-1 dependent amyloid precursor protein translation: implications for down syndrome and Alzheimer's disease. *PLoS ONE* **8**, e65978 (2013).
209. Utsuki, T. et al. Identification of novel small molecule inhibitors of amyloid precursor protein synthesis as a route to lower Alzheimer's disease amyloid-beta peptide. *J. Pharmacol. Exp. Ther.* **318**, 855–862 (2006).
210. Canzoneri, J. C. & Oyelere, A. K. Interaction of anthracyclines with iron responsive element mRNAs. *Nucleic Acids Res.* **36**, 6825–6834 (2008).
211. Venti, A. et al. The integrated role of desferrioxamine and phenesine targeted to an iron-responsive element in the APP-mRNA 5'-untranslated region. *Ann. N. Y. Acad. Sci.* **1035**, 34–48 (2004).
212. Tibodeau, J. D., Fox, P. M., Ropp, P. A., Theil, E. C. & Thorp, H. H. The up-regulation of ferritin expression using a small-molecule ligand to the native mRNA. *Proc. Natl. Acad. Sci. USA* **103**, 253–257 (2006).
213. Cahill, C. M., Aleyadeh, R., Gao, J., Wang, C. & Rogers, J. T. Alpha-synuclein in alcohol use disorder, connections with Parkinson's disease and potential therapeutic role of 5' untranslated region-directed small molecules. *Biomolecules* **10**, 1465 (2020).
214. Stefanis, L. alpha-Synuclein in Parkinson's disease. *Cold Spring Harb. Perspect. Med.* **2**, a009399 (2012).
215. Rocha, E. M., De Miranda, B. & Sanders, L. H. Alpha-synuclein: pathology, mitochondrial dysfunction and neuroinflammation in Parkinson's disease. *Neurobiol. Dis.* **109**, 249–257 (2018).
216. Junn, E. et al. Repression of alpha-synuclein expression and toxicity by microRNA-7. *Proc. Natl. Acad. Sci. USA* **106**, 13052–13057 (2009).
217. Ule, J. & Blencowe, B. J. Alternative splicing regulatory networks: functions, mechanisms, and evolution. *Mol. Cell.* **76**, 329–345 (2019).
218. Lee, Y. & Rio, D. C. Mechanisms and regulation of alternative pre-mRNA splicing. *Annu. Rev. Biochem.* **84**, 291–323 (2015).
219. Bauman, J., Jearwairiyapaisarn, N. & Kole, R. Therapeutic potential of splice-switching oligonucleotides. *Oligonucleotides* **19**, 1–13 (2009).
220. Sazani, P. & Kole, R. Therapeutic potential of antisense oligonucleotides as modulators of alternative splicing. *J. Clin. Invest.* **112**, 481–486 (2003).
221. Havens, M. A. & Hastings, M. L. Splice-switching antisense oligonucleotides as therapeutic drugs. *Nucleic Acids Res.* **44**, 6549–6563 (2016).
222. Scharner, J. et al. Hybridization-mediated off-target effects of splice-switching antisense oligonucleotides. *Nucleic Acids Res.* **48**, 802–816 (2020).
223. Arendt, T., Stieler, J. T. & Holzer, M. Tau and tauopathies. *Brain Res. Bull.* **126**, 238–292 (2016).
224. Donahue, C. P., Muratore, C., Wu, J. Y., Kosik, K. S. & Wolfe, M. S. Stabilization of the tau exon 10 stem loop alters pre-mRNA splicing. *J. Biol. Chem.* **281**, 23302–23306 (2006).
225. Zheng, S., Chen, Y., Donahue, C. P., Wolfe, M. S. & Varani, G. Structural basis for stabilization of the tau pre-mRNA splicing regulatory element by novantrone (mitoxantrone). *Chem. Biol.* **16**, 557–566 (2009).
226. Lisowiec, J., Magnier, D., Kierzek, E., Lenartowicz, E. & Kierzek, R. Structural determinants for alternative splicing regulation of the MAPT pre-mRNA. *RNA Biol.* **12**, 330–342 (2015).
227. Liu, Y. et al. Mitoxantrone analogues as ligands for a stem-loop structure of tau pre-mRNA. *J. Med. Chem.* **52**, 6523–6526 (2009).
228. Luo, Y. & Disney, M. D. Bottom-up design of small molecules that stimulate exon 10 skipping in mutant MAPT pre-mRNA. *Chembiochem* **15**, 2041–2044 (2014).
229. Sakamoto, K. M. et al. Protacs: chimeric molecules that target proteins to the Skp1-Cullin-F box complex for ubiquitination and degradation. *Proc. Natl. Acad. Sci. USA* **98**, 8554–8559 (2001).
230. Zou, Y., Ma, D. & Wang, Y. The PROTAC technology in drug development. *Cell Biochem. Funct.* **37**, 21–30 (2019).
231. Sakamoto, K. M. Chimeric molecules to target proteins for ubiquitination and degradation. *Methods Enzymol.* **399**, 833–847 (2005).
232. Ottis, P. & Crews, C. M. Proteolysis-targeting chimeras: induced protein degradation as a therapeutic strategy. *ACS Chem. Biol.* **12**, 892–898 (2017).
233. Crews, C. M. Inducing protein degradation as a therapeutic strategy. *J. Med. Chem.* **61**, 403–404 (2018).
234. Chamberlain, P. P. & Hamann, L. G. Development of targeted protein degradation therapeutics. *Nat. Chem. Biol.* **15**, 937–944 (2019).
235. Costales, M. G., Suresh, B., Vishnu, K. & Disney, M. D. Targeted degradation of a hypoxia-associated non-coding RNA enhances the selectivity of a small molecule interacting with RNA. *Cell Chem. Biol.* **26**, 1180–1186 (2019).
236. Thakur, C. S. et al. Small-molecule activators of RNase L with broad-spectrum antiviral activity. *Proc. Natl. Acad. Sci. USA* **104**, 9585–9590 (2007).
237. Janes, J. et al. The ReFRAME library as a comprehensive drug repurposing library and its application to the treatment of cryptosporidiosis. *Proc. Natl. Acad. Sci. USA* **115**, 10750–10755 (2018).
238. Grundy, F. J. & Henkin, T. M. The S box regulon: a new global transcription termination control system for methionine and cysteine biosynthesis genes in Gram-positive bacteria. *Mol. Microbiol.* **30**, 737–749 (1998).
239. Gelfand, M. A conserved RNA structure element involved in the regulation of bacterial riboflavin synthesis genes. *Trends Genet.* **15**, 439–442 (1999).
240. Mironov, A. S. et al. Sensing small molecules by nascent RNA. *Cell* **111**, 747–756 (2002).
241. Nahvi, A. et al. Genetic control by a metabolite binding mRNA. *Chem. Biol.* **9**, 1043–1049 (2002).
242. Winkler, W., Nahvi, A. & Breaker, R. R. Thiamine derivatives bind messenger RNAs directly to regulate bacterial gene expression. *Nature* **419**, 952–956 (2002).
243. Winkler, W. C. & Breaker, R. R. Regulation of bacterial gene expression by riboswitches. *Annu. Rev. Microbiol.* **59**, 487–517 (2005).
244. Polaski, J. T., Kletzien, O. A., Drogalis, L. K. & Batey, R. T. A functional genetic screen reveals sequence preferences within a key tertiary interaction in cobalamin riboswitches required for ligand selectivity. *Nucleic Acids Res.* **46**, 9094–9105 (2018).
245. Batey, R. T., Gilbert, S. D. & Montange, R. K. Structure of a natural guanine-responsive riboswitch complexed with the metabolite hypoxanthine. *Nature* **432**, 411–415 (2004).
246. Batey, R. T., Rambo, R. P. & Doudna, J. A. Tertiary motifs in RNA structure and folding. *Angew. Chem. Int. Ed. Engl.* **38**, 2326–2343 (1999).
247. Breaker, R. R. Riboswitches and the RNA world. *Cold Spring Harb. Perspect. Biol.* **4**, a003566 (2012).
248. Garst, A. D., Edwards, A. L. & Batey, R. T. Riboswitches: structures and mechanisms. *Cold Spring Harb. Perspect. Biol.* **3**, a003533 (2011).
249. Sherlock, M. E. & Breaker, R. R. Former orphan riboswitches reveal unexplored areas of bacterial metabolism, signaling, and gene control processes. *RNA* **26**, 675–693 (2020).
250. Wang, J. X. & Breaker, R. R. Riboswitches that sense S-adenosylmethionine and S-adenosylhomocysteine. *Biochem. Cell. Biol.* **86**, 157–168 (2008).
251. Balibar, C. J. et al. Validation and development of an *Escherichia coli* riboflavin pathway phenotypic screen hit as a small-molecule ligand of the flavin mononucleotide riboswitch. *Methods Mol. Biol.* **1787**, 19–40 (2018).
252. Serganov, A., Huang, L. & Patel, D. J. Coenzyme recognition and gene regulation by a flavin mononucleotide riboswitch. *Nature* **458**, 233–237 (2009).
253. Vicens, Q., Mondragón, E. & Batey, R. T. Molecular sensing by the aptamer domain of the FMN riboswitch: a general model for ligand binding by conformational selection. *Nucleic Acids Res.* **39**, 8586–8598 (2011). **A structural analysis of FMN binding to the FMN riboswitch using SHAPE mapping and X-ray crystallography reveals detailed conformational changes upon ligand binding.**
254. Blount, K. F. et al. Novel riboswitch-binding flavin analog that protects mice against *Clostridium difficile* infection without inhibiting cecal flora. *Antimicrob. Agents Chemother.* **59**, 5736–5746 (2015).
255. Vicens, Q. et al. Structure–activity relationship of flavin analogues that target the flavin mononucleotide riboswitch. *ACS Chem. Biol.* **13**, 2908–2919 (2018).
256. Cho, S. & Dreyfuss, G. A degron created by SMN2 exon 7 skipping is a principal contributor to spinal muscular atrophy severity. *Genes Dev.* **24**, 438–442 (2010).
257. Ratni, H. et al. Specific correction of alternative survival motor neuron 2 splicing by small molecules: discovery of a potential novel medicine to treat spinal muscular atrophy. *J. Med. Chem.* **59**, 6086–6100 (2016).
258. Campagne, S. et al. Structural basis of a small molecule targeting RNA for a specific splicing correction. *Nat. Chem. Biol.* **15**, 1191–1198 (2019).
259. Sivaramakrishnan, M. et al. Binding to SMN2 pre-mRNA–protein complex elicits specificity for small molecule splicing modifiers. *Nat. Commun.* **8**, 1476 (2017).
260. Wang, J., Schultz, P. G. & Johnson, K. A. Mechanistic studies of a small-molecule modulator of SMN2 splicing. *Proc. Natl. Acad. Sci. USA* **115**, E4604–E4612 (2018).
261. Keller, C. G. et al. An orally available, brain penetrant, small molecule lowers huntingtin levels by enhancing pseudoexon inclusion. *Nat. Commun.* **13**, 1150 (2022).
262. Chaidir, C., Edrada-Ebel, R., Ebel, R., Bohnenstengel, F. & Nugroho, B. W. Chemistry and biological activity of rocaglamide derivatives and related compounds in *Aglaia* species (Meliaceae). *Curr. Org. Chem.* **5**, 923–938 (2001).
263. Kim, S. et al. Silvestrol, a potential anticancer rocaglate derivative from *Aglaia foveolata*, induces apoptosis in LNCaP cells through the mitochondrial/apoptosome pathway without activation of executioner caspase-3 or -7. *Anticancer Res.* **27**, 2175–2183 (2007).
264. Schulz, G., Victoria, C., Kirschning, A. & Steinmann, E. Rocaglamide and silvestrol: a long story from anti-tumor to anti-coronavirus compounds. *Nat. Prod. Rep.* **38**, 18–23 (2021).
265. Iwasaki, S., Floor, S. N. & Ingolia, N. T. Rocaglates convert DEAD-box protein eIF4A into a sequence-selective translational repressor. *Nature* **534**, 558–561 (2016). **A mechanistic study showing that the anti-tumour drug rocaglamide A functions by clamping eIF4A to purine sequences and blocking ribosomal scanning in the 5' UTR.**
266. Ernst, J. T. et al. Design of development candidate eFT226, a first in class inhibitor of eukaryotic initiation factor 4A RNA helicase. *J. Med. Chem.* **63**, 5879–5955 (2020).
267. Nileske, C. et al. 1-Aminomethyl SAR in a novel series of flavagline-inspired eIF4A inhibitors: effects of amine substitution on cell potency and in vitro PK properties. *Bioorg. Med. Chem. Lett.* **47**, 128111 (2021).
268. Nileske, C. et al. Strategic diastereoselective C1 functionalization in the aza-rocaglamide scaffold toward natural product-inspired eIF4A inhibitors. *Org. Lett.* **22**, 6257–6261 (2020).
269. Kruger, K. et al. Self-splicing RNA: autoexcision and autocyclization of the ribosomal RNA intervening sequence of *Tetrahymena*. *Cell* **31**, 147–157 (1982).
270. Guerrer-Takada, C., Gardiner, K., Marsh, T., Pace, N. & Altman, S. The RNA moiety of ribonuclease P is the catalytic subunit of the enzyme. *Cell* **35**, 849–857 (1983).
271. Cech, T. R. & Bass, B. L. Biological catalysis by RNA. *Annu. Rev. Biochem.* **55**, 599–629 (1986).
272. Peattie, D. A., Douthwaite, S., Garrett, R. A. & Noller, H. F. A "bulged" double helix in a RNA–protein contact site. *Proc. Natl. Acad. Sci. USA* **78**, 7331–7335 (1981).
273. Moazed, D. & Noller, H. F. Interaction of antibiotics with functional sites in 16S ribosomal RNA. *Nature* **327**, 389–394 (1987).
274. Velagapudi, S. P., Li, Y. & Disney, M. D. A cross-linking approach to map small molecule–RNA binding sites in cells. *Bioorg. Med. Chem. Lett.* **29**, 1532–1536 (2019).
275. Lipinski, C. A., Lombardo, F., Dominy, B. W. & Feeney, P. J. Experimental and computational approaches to estimate solubility and permeability in drug discovery and development settings. *Adv. Drug Deliv. Rev.* **46**, 3–26 (2001).
276. Davila-Calderon, J. et al. IRES-targeting small molecule inhibits enterovirus 71 replication via allosteric stabilization of a ternary complex. *Nat. Commun.* **11**, 4775 (2020).
277. Liu, T. & Pyle, A. M. Discovery of highly reactive self-splicing group II introns within the mitochondrial genomes of human pathogenic fungi. *Nucleic Acids Res.* **49**, 12422–12432 (2021).
278. Angelbello, A. J. et al. Precise small-molecule cleavage of an r(CUC) repeat expansion in a myotonic dystrophy mouse model. *Proc. Natl. Acad. Sci. USA* **116**, 7799–7804 (2019).
279. Donahue, C. P., Ni, J., Rozners, E., Glicksman, M. A. & Wolfe, M. S. Identification of tau stem loop RNA stabilizers. *J. Biomol. Screen.* **12**, 789–799 (2007).

280. Angelbello, A. J. et al. A small molecule that binds an RNA repeat expansion stimulates its decay via the exosome complex. *Cell Chem. Biol.* **28**, 34–45 (2021). **Demonstrates that RNA-targeting small molecules can interface the target with natural decay pathways, in particular the exosome.**
281. Murchie, A. I. et al. Structure-based drug design targeting an inactive RNA conformation: exploiting the flexibility of HIV-1 TAR RNA. *J. Mol. Biol.* **336**, 625–638 (2004).
282. Foloppe, N. et al. A structure-based strategy to identify new molecular scaffolds targeting the bacterial ribosomal A-site. *Bioorg. Med. Chem.* **12**, 935–947 (2004).
283. Morgan, B. S., Forte, J. E., Culver, R. N., Zhang, Y. & Hargrove, A. E. Discovery of key physicochemical, structural, and spatial properties of RNA-targeted bioactive ligands. *Angew. Chem. Int. Ed. Engl.* **56**, 13498–13502 (2017).
284. Childs-Diasney, J. L. et al. A massively parallel selection of small molecule–RNA motif binding partners informs design of an antiviral from sequence. *Chem.* **4**, 2384–2404 (2018).
285. Bickerton, G. R., Paolini, G. V., Besnard, J., Muresan, S. & Hopkins, A. L. Quantifying the chemical beauty of drugs. *Nat. Chem.* **4**, 90–98 (2012).
286. Bhullar, K. S. et al. Kinase-targeted cancer therapies: progress, challenges and future directions. *Mol. Cancer* **17**, 48 (2018).
287. Paulson, H. Repeat expansion diseases. *Handb. Clin. Neurol.* **147**, 105–123 (2018).
288. Bernat, V. & Disney, M. D. RNA structures as mediators of neurological diseases and as drug targets. *Neuron* **87**, 28–46 (2015).
289. de Mezer, M., Wojciechowska, M., Napierala, M., Sobczak, K. & Krzyzosiak, W. J. Mutant CAG repeats of huntingtin transcript fold into hairpins, form nuclear foci and are targets for RNA interference. *Nucleic Acids Res.* **39**, 3852–3863 (2011).
290. Sobczak, K., de Mezer, M., Michlewski, G., Krol, J. & Krzyzosiak, W. J. RNA structure of trinucleotide repeats associated with human neurological diseases. *Nucleic Acids Res.* **31**, 5469–5482 (2003).
291. Tian, B. et al. Expanded CUG repeat RNAs form hairpins that activate the double-stranded RNA-dependent protein kinase PKR. *RNA* **6**, 79–87 (2000).
292. Jog, S. P. et al. RNA splicing is responsive to MBNL1 dose. *PLoS ONE* **7**, e48825 (2012).
293. Rzuczek, S. G. et al. Precise small-molecule recognition of a toxic CUG RNA repeat expansion. *Nat. Chem. Biol.* **13**, 188–193 (2017).
294. Wagner-Griffin, S. et al. A druglike small molecule that targets r(CCUG) repeats in myotonic dystrophy type 2 facilitates degradation by RNA quality control pathways. *J. Med. Chem.* **64**, 8474–8485 (2021).
295. Bush, J. A. et al. Ribonuclease recruitment using a small molecule reduced c9ALS/FTD r(G,C<sub>2</sub>) repeat expansion *in vitro* and *in vivo* ALS models. *Sci. Transl. Med.* **13**, eabd5991 (2021).
296. Angelbello, A. J. & Disney, M. D. A toxic RNA templates the synthesis of its own fluorogenic inhibitor by using a bio-orthogonal tetrazine ligation in cells and tissues. *ACS Chem. Biol.* **15**, 1820–1825 (2020).
297. Burma, S., Chen, B. P., Murphy, M., Kurimasa, A. & Chen, D. J. ATM phosphorylates histone H2AX in response to DNA double-strand breaks. *J. Biol. Chem.* **276**, 42462–42467 (2001).
298. Li, Y. & Disney, M. D. Precise small molecule degradation of a noncoding RNA identifies cellular binding sites and modulates an oncogenic phenotype. *ACS Chem. Biol.* **13**, 3065–3071 (2018).
299. Liu, X. et al. Targeted degradation of the oncogenic microRNA 17-92 cluster by structure-targeting ligands. *J. Am. Chem. Soc.* **142**, 6970–6982 (2020).
300. Benhamou, R. I. et al. Structure-specific cleavage of an RNA repeat expansion with a dimeric small molecule is advantageous over sequence-specific recognition by an oligonucleotide. *ACS Chem. Biol.* **15**, 485–493 (2020).

**Acknowledgements**

This work was funded by the NIH (R35 NS116846, R01 CA249180, UG3 NS116921 and P01 NS099114 to M.D.D. and R01 GM073850 to R.T.B.) and the Department of Defense (W81XWH-19-1-0719 and W81XWH-20-1-0727 to M.D.D.).

**Author contributions**

All authors contributed to the writing of the manuscript and preparation of figures.

**Competing interests**

M.D.D. is a founder of Expansion Therapeutics. R.T.B. serves on the Scientific Advisory Board of Expansion Therapeutics and MeiraGTx. The remaining authors declare no competing interests.

**Publisher's note**

Springer Nature remains neutral with regard to jurisdictional claims in published maps and institutional affiliations.

Springer Nature or its licensor holds exclusive rights to this article under a publishing agreement with the author(s) or other rightsholder(s); author self-archiving of the accepted manuscript version of this article is solely governed by the terms of such publishing agreement and applicable law.

© Springer Nature Limited 2022